A comprehensive and systematic diagnostic campaign for a new acquisition of contemporary art—the case of Natura Morta by Andreina Rosa (1924–2019) at the

heritage

MDPI

Article

A Comprehensive and Systematic Diagnostic Campaign for a New Acquisition of Contemporary Art—The Case of *Natura Morta* by Andreina Rosa (1924–2019) at the International Gallery of Modern Art Ca' Pesaro, Venice

Anna Piccolo [1], Emanuele Bonato [1], Laura Falchi [1], Paola Lucero-Gómez [1], Elisabetta Barisoni [2], Matteo Piccolo [2], Eleonora Balliana [1], Dafne Cimino [1] and Francesca Caterina Izzo [1,*]

[1] Sciences and Technologies for the Conservation of Cultural Heritage, Department of Environmental Sciences, Informatics and Statistics, Ca' Foscari University of Venice, Via Torino 155/b, 30173 Venice, Italy; 870194@stud.unive.it (A.P.); 974901@stud.unive.it (E.B.); laura.falchi@unive.it (L.F.); paola.lucero@unive.it (P.L.-G.); eleonora.balliana@unive.it (E.B.); dafne.cimino@unive.it (D.C.)

[2] Fondazione Musei Civici, MUVE—Galleria Internazionale d'Arte Moderna di Ca' Pesaro, Santa Croce 2076, 30135 Venice, Italy; elisabetta.barisoni@fmcvenezia.it (E.B.); matteo.piccolo@fmcvenezia.it (M.P.)

* Correspondence: fra.izzo@unive.it

check for updates

Citation: Piccolo, A.; Bonato, E.; Falchi, L.; Lucero-Gómez, P.; Barisoni, E.; Piccolo, M.; Balliana, E.; Cimino, D.; Izzo, F.C. A Comprehensive and Systematic Diagnostic Campaign for a New Acquisition of Contemporary Art—The Case of *Natura Morta* by Andreina Rosa (1924–2019) at the International Gallery of Modern Art Ca' Pesaro, Venice. *Heritage* **2021**, *4*, 4372–4398. https://doi.org/10.3390/heritage4040242

Academic Editor: João Pedro Veiga

Received: 30 August 2021
Accepted: 13 November 2021
Published: 16 November 2021

Abstract: A multi-analytical approach has been employed to investigate the painting Natura Morta (1954–1955) by Andreina Rosa (1924–2019) to assess the state of conservation and to understand more about the painting materials and techniques of this artwork, which was recently donated by the painter's heirs to the International Gallery of Modern Art Ca' Pesaro (Venice-Italy). A comprehensive and systematic diagnostic campaign was carried out, mainly adopting non-invasive imaging and spectroscopic methods, such as technical photography, optical microscopy, Hyperspectral Imaging Spectroscopy (HIS), fiber optics reflectance spectroscopy (FORS), External Reflectance Fourier Transform Infrared (ER-FTIR), and Raman spectroscopies. Microsamples, collected from the edges of the canvas in areas partially detached, were studied by Attenuated Total Reflection Fourier Transform Infrared (ATR-FTIR) spectroscopy and Gas Chromatography-Mass Spectrometry (GC-MS). By crossing the information gained, it was possible to make inferences about the composition of the groundings and the painted layers, the state of conservation of the artwork, and the presence of degradation phenomena. Hence, the present study may be of interest for conservation purposes as well as for enhancing the artistic activity of Andreina Rosa. The final aim was to provide useful information for the Gallery which recently included this painting in its permanent collection.

Keywords: Andreina Rosa; heritage science; modern oil painting; conservation; oxalates; GC-MS; Hyperspectral Imaging Spectroscopy; FORS; ER-FTIR; degradation

1. Introduction

Andreina Rosa (1924–2019), daughter of a goldsmith and sculptor, was a renowned Venetian artist, who, besides painting, also experimented with decorative and applied arts such as mosaics and lacquers. Combining artistic practice with teaching, she took part in prestigious art competitions and exhibitions, such as the Quadriennale in Rome and the Art Biennale in Venice, where she was present in all the editions between 1950 and 1970s [1,2]. After her death in 2019, some of her artworks, stored in the heirs' households, were donated to the International Gallery of Modern Art Ca' Pesaro in Venice (Italy), which is part of the Fondazione Musei Civici (MUVE). After arriving at the museum in 2020, they were catalogued and became part of the permanent collection. In the framework of the research agreement between MUVE and the research group of "Heritage and Conservation Science" at the Ca' Foscari University of Venice, seven paintings were entrusted to the

heritage scientists for a diagnostic study in the timeframe between March and May 2021. In the present work, the research on one emblematic painting by Andreina Rosa is discussed.

The artwork under investigation is titled *Natura Morta*, was painted around 1954–1955, and is provisionally catalogued as an oil painting. The major goals of the technical study consisted in deepening the knowledge about the state of conservation, the composition of the painted layers, and the painting technique by using a multi-analytical approach. The choice of *Natura Morta* has been dictated by the worse condition in which the work was compared to the other six paintings and therefore studied in a deeper way to better understand the problems highlighted (see Section 3.1, *State of conservation and degradation phenomena*).

Investigations on contemporary artworks may be quite challenging as painters started using rather complex commercial paint formulations or experimenting by mixing even products that were not intended for artistic purposes [3–9]. In the last decade, several studies have underlined a possible correlation among paint compositions and degradation phenomena observed in oil paintings (such as binder separation, exudations, extensive craquelures, water, and solvent sensitivity, etc.) [9–14]. Thus, the importance of widening the knowledge of commercial painting materials and understanding the behaviour over time of the resulting painting systems is evident.

In this work, next to direct visual observations, macro- and micro- observations were performed with the help of technical photography and microscopes, while a compositional study was developed by employing various spectroscopic techniques. In order to preserve the integrity of the painting, mainly non-invasive spectroscopic techniques were employed using portable instruments. These were Hyperspectral Imaging Spectroscopy (HIS), Fiber Optics Reflectance Spectroscopy (FORS), External Reflectance Fourier Transform Infrared (ER-FTIR), and Raman spectroscopies.

The painting, in fact, was crossed by widespread and extensive cracks and the manipulation of the artwork itself required careful attention in order not to risk the loss of micro-fragments of the pictorial layers. Where, however, such paint falls were unavoidable (especially from the edges), the collected micro-fragments were studied through destructive analyses, such as Attenuated Total Reflection Fourier Transform Infrared (ATR-FTIR) spectroscopy and Gas Chromatography-Mass Spectrometry (GC-MS).

The combination of all these techniques was the basis for developing the present multi-analytical study: a fruitful discussion of the results obtained may both implement the knowledge on Andreina Rosa's painting and allow us to draw useful conclusions for the conservation and musealization of the work of art.

2. Materials and Methods

2.1. Macro- and Micro-Observation

The very first investigation to be made on the painting consisted of direct visual observation: a fundamental step to observe and report every detail that might not be evident at first glance.

2.1.1. Technical Photography

Being completely non-invasive, investigations through technical photography have been performed as one of the first analyses on the painting. Photographs in the visible range and with IR filters were taken outdoors during the daytime. Three high-pass filters—at 720, 850, and 950 nm—were used for IR reflectography. For UV-induced fluorescence, transillumination, and raking light images acquisitions, the painting was placed in a dark room in order to illuminate it just with the radiation of the proper type and direction. The employed UV sources were purchased from MADAtec Srl (Italy) and had a power output of ca. 3 W and the emission peak at 365 nm. A Nikon D5600 was used for all the acquisitions except for IR technical photography. For the latter a Samsung NX3300 camera (modified by MADAtec Srl) was employed, equipped with Hoya filters.

2.1.2. Optical Microscopy

Microscopic observations on the canvas were carried out using a DINO-lite digital microscope, both using visible and UV illumination. The acquired images have been processed with DinoCapture 2.0 software, and the instrument was calibrated before each usage, for a 55x magnification. Micro-samples detached from the painting were observed magnified with the help of an Optika microscope, equipped with two kinds of high-pass filters at 505 nm and 535 nm (visible in Appendix A, Figure A1).

The canvas fibers were identified by means of an optical transmission microscope by Optika.

2.2. Spectroscopic Analyses

Different spectroscopic techniques have been used for questioning the composition of the painted and the preparation layers. Areas with quite homogeneous colors were selected for the identification of the pigments and are described in Figure 1.

Figure 1. Areas analyzed with the different spectroscopic techniques for the study of the painted layers. To each of them, an optical 55× magnification image is associated together with the assigned name. In these, the numbers have no function other than distinguishing the areas.

Hyperspectral imaging was performed with a portable Hyperspectral Camera Specim IQ, which collected images and reflectance spectra of the whole artwork and some details in the spectral range from 400 to 1000 nm. Data were elaborated with Specim IQ studio software, which allows the creation of masks to highlight areas with similar spectral features based upon the variance of the spectra collected (pi value). This way, the portions of the painting containing presumably the same pigments can be recognized thanks to the false color image overlapped with the visible picture.

FORS analyses were performed on all the fifteen areas shown in the map of Figure 1 using an ASD FieldSpec 4 Standard—Res Spectroradiometer equipped with three detectors, working in the range between 350 and 2500 nm (resolution of 3 nm in the Vis-Near IR range 350–1000 nm, 8 nm in the SWIR 1000–1800, and 1800–2500 nm) and endowed with a contact probe with an inner halogen light source collecting light scattered at 45° and a spot size of 1.2 cm^2. The spectra were obtained as average of three acquisitions. For data elaboration, ViewSpec Pro software and Origin 8.5 were employed. Identification of

pigments was based on the CNR-IFAC database [15], the comparison with spectral data from US geological service [16], and specific literature [17–19].

A Bruker ALPHA II Fourier Transform IR Spectrometer was used for External-Reflection (ER-FTIR) and ATR-FTIR analysis. ER-FTIR analyses were performed using an aperture of 6 mm and a 3 min of acquisition time. These measurements allowed for the registration of spectra in the range 7500 ÷ 350 cm^{-1}, which comprises wavenumbers where combination bands and overtones are present. Blue 1, Yellow 7, Brown 10, White 11, and Grey 12 could not be analyzed through this technique due to practical constraints in the measurement settings. ATR-FTIR analysis were recorded in the spectral range from 4000 to 350 cm^{-1}, using a synthetic diamond crystal for the compression of the samples. The background was measured with 24 scans before each acquisition, while samples were investigated using 128 scans, 4 cm^{-1} resolution.

Raman spectra were collected with a Bravo portable Raman spectrometer by Bruker Optics, characterized by a dual laser excitation (two lasers at 758 and 852 nm working simultaneously). The Ramanspectra were collected in the 3200–300 cm^{-1} spectral range between, with 10 cm^{-1} resolution, scan time from 1 s to 60 s. Measurements were carried out on all the colors considered with the other spectroscopic techniques, except from *Grey 12*, since, based on the results already obtained, such hue was determined to be probably a mixture of pigments present in other analyzed areas.

OPUS software managed the acquisition and elaboration of IR and Raman spectra. The data were further elaborated with Origin 8.5.

2.3. Gas Chromatography/Mass Spectrometry (GC/MS)

Gas Chromatography-Mass Spectrometry (GC-MS) analysis was performed on micro-samples from detached areas to elucidate the nature of the lipidic binding media.

For each sample, a mass of ca. 0.10 mg was treated with 30 uL of m(trifluoromethylphenyl) trimethylammonium hydroxide, 2.5% in methanol, overnight reaction at room temperature, as described in [3,5,20–23]. Then, 1 uL of each derivatized sample was automatically injected by an AS1310 autosampler (Thermoscientific) in a Trace GC 1300 system equipped with a MS detector ISQ 7000 with a quadrupole analyzer (Thermoscientific). The GC separation was performed on a chemically bonded fused silica capillary DB–5MS Column (30 m length, 0.25 mm, 0.25 um—5% phenyl methyl polysiloxane), using helium as the carrier gas (flow rate 1 mL/min). The inlet temperature was 280 °C, and the MS interface was at 280 °C. The transfer line was at 280 °C and the MS source temperature was 300 °C. The temperature program ranged from 50 (held 2 min) to 320 °C (held 5 min) with a ramp of 10 °C/min. The MS was run in full scan mode (m/z 40–650), 1.9 scans/s. Electron ionization energy was 70 eV.

The identification of the compounds was done by comparison with the NIST and MS Search 1.7 libraries of mass spectra and a library created by the authors.

Quantitative analysis was achieved using nonadecanoic acid as the internal standard and a standard solution containing saturated and unsaturated fatty acids and glycerol. The molar ratios among the most important fatty acids were calculated: A/P (azelaic to palmitic acid ratio), to provide information on the degree of oxidation of oil; P/S (palmitic to stearic acid ratio) is commonly used to suggest the type of drying oils; O/S (oleic to stearic acid ratio) may indicate the maturity of oils (i.e., the amount of remaining unsaturated fatty acids) [24–27].

3. Results

3.1. State of Conservation and Degradation Phenomena

By observing the painting *Natura Morta*, it can be noticed that the depictions continue along the sides and the borders of the canvas present signs of raveling: such evidence suggests that originally the artwork was larger and was subsequently redimensioned on the present stretchers.

The support on which the canvas is fixed is probably handmade, as the wooden stretchers appear rather rough and uneven: there are knots in the wood and several signs of manipulation can be seen. The presence of a manufacturer's name label and some remnants of what may have been a price tag support this hypothesis.

The fixing was done with nails and was reinforced with glue on the upper edge (see Figure A2 in Appendix B). Observing with the help of a UV light, traces of glue were also present on the edges of the painting (resulting in a greenish fluorescence), probably traces of the adhesive used for lining the artwork. A piece of paper, in fact, was found under a pin attached to the top edge and was covered by an adhesive material on the side that faced the painting. The lining was likely torn, resulting in widespread losses on the edges. Based on the analysis performed, it is still unclear whether the adhesives used for the mentioned purposes coincide or differ.

The Raman spectrum obtained for the glue present on the upper edge was characterized by a sharp and strong peak at 2938 cm^{-1}: this is attributed to the C-H stretching mode and, together with the C=O stretching signal at 1736 cm^{-1}, could suggest the presence of polyvinyl acetate-based glue [28]. Based on the ATR-FTIR results for the adhesive remnants on the piece of paper, instead, it could be hypothesized that an aged synthetic rubber glue was present. Characteristic signals were detected at 1713 cm^{-1} (υ C=O), 1448 cm^{-1} and 1399 cm^{-1} (CH_2 and CH_3), in the region around 1100–1000 cm^{-1} (C-O-C ether group) and at 744 cm^{-1} and 700 cm^{-1} (aromatic groups) [29].

The cutting out and transfer to the new wooden support of the canvas severely compromised the mechanical stability and is probably the main cause of the formation of cracks. These are diffused both along the edges of the painting, where the canvas has been folded (Figure 2a), and in correspondence with the points of pinning of the nails. Here, the elongated pattern of the cracks seems to follow the axes of mechanical tension (Figure 2b). An extensive craquelure that crosses the entire painting on its left side can also be attributed to the stretching of the work in its adaptation on the new support, since its shape corresponds to the undulation of the underlying canvas.

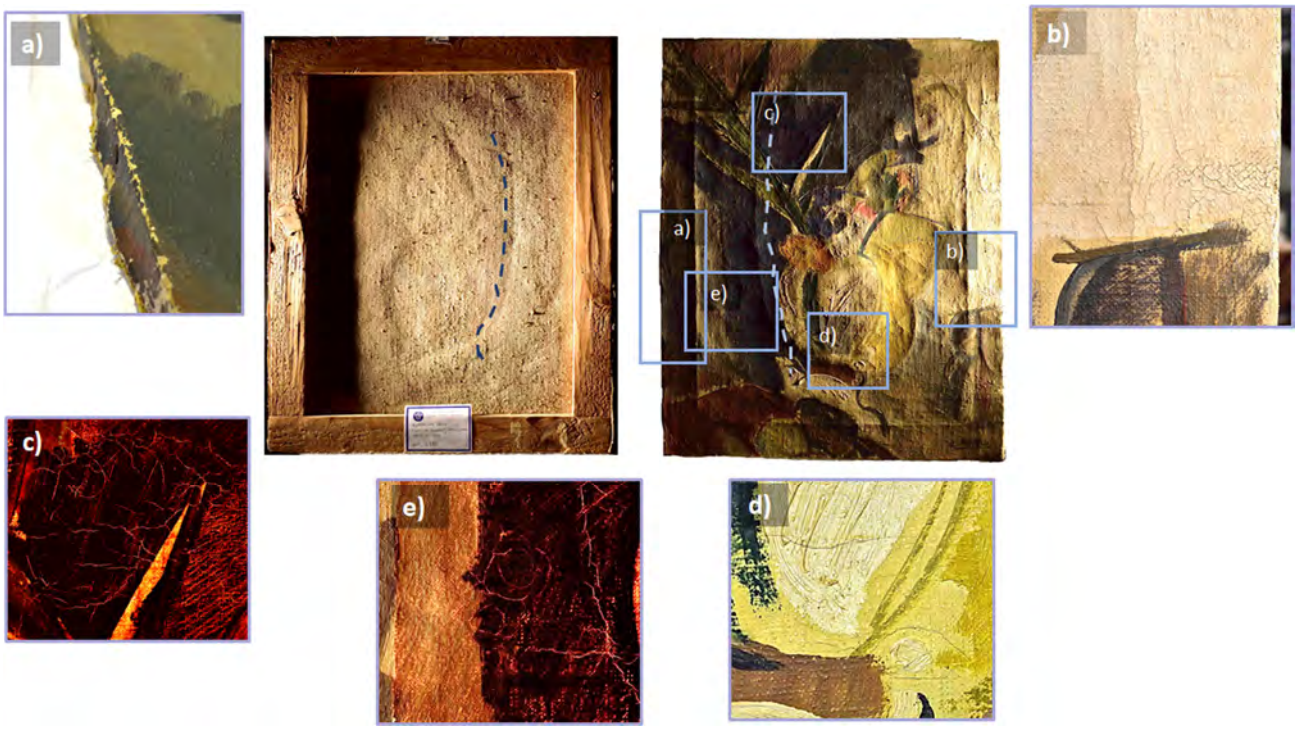

Figure 2. Raking light photographs of the back and front of the painting and details of peculiar cracks (**a**) along the edge; (**b**) in correspondence with the stretcher border and the nail pinning; (**c**) widespread (seen with transillumination); (**d**) crossing and surrounding thick painted areas; (**e**) due to local impacts from handling (transillumination).

The warp of the canvas is evidently distorted, due to the fixing with nails on opposite edges, so the cracks have preferentially formed along the threads that have been most stretched in that process, as is the case of the one evidenced with the blue dashed line in Figure 2. Not only are the cracks present because of the traumatic event mentioned, but they also arise diffusely on the painting because of other complex dynamics among the artwork's materials and the surrounding environment. In particular, fluctuations in humidity and temperature and the resulting movements of different compounds in the paints likely played a role. As has been observed by Fuster-López et al. on a series of Picasso paintings [30,31], a strong mechanical stress arises when the two opposing forces—of swelling of the hygroscopic materials on the one hand and of confining the space through the limits of the support on the other—collide.

In *Natura Morta* several moisture-sensitive materials are present: animal glue and gypsum in the preparation layer, as well as the wooden support and the canvas fabric. The canvas is made of cotton, identified by the characteristic smooth and twisted shape of the fibers (Figure 3a), and therefore highly hygroscopic [32,33]. Mechanical stresses emerged from the opposition of a contrasting force to such movements given by both the anchorage on the support and the tightly woven canvas: the covering factor resulted to be ca. 75% (Figure 3b) [32–36]. As a result, craquelures formed widely over the painting as an intricate network extending in all directions. While only a limited portion of them could be seen by direct visual observation, using transillumination it was possible to highlight their copiousness throughout the surface (Figure 2c). The changes in environmental conditions, to which the artwork was probably exposed during its conservation in the houses of Rosa's heirs, also affected the painting on a larger scale by determining a loosening of the canvas: it bent at the edges of the stretchers so that craquelures formed along the wooden bars.

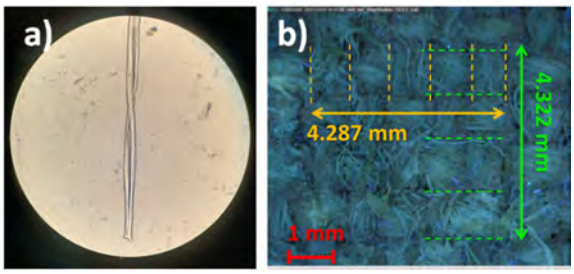

Figure 3. (**a**) Optical-microscopy photograph of the fiber of the canvas observed with transmitted light; (**b**) microscopy photograph of the woven canvas (back of the painting) taken with DINO light with UV light and a 55× magnification.

Some cracks were also observed in isolated or precisely spatially confined parts and were probably not associated with mechanical stress, but with some brushstrokes (Figure 2d). They were likely caused by the different drying rates for the distinct painted areas. Differential drying of the brushstrokes, due to thickness or level of paint dilution, resulted in a very complex and heterogeneous morphology on the studied work, with protuberances and depressions for the distinct painted areas. This is dramatically appreciable when observing the front of the artwork with raking light but is also noticeable when considering the back side (Figure 2).

Other isolated cracks were observed in an area where the painted layer was fairly homogeneous. These have a rounded pattern (Figure 2e) and probably originated due to local impacts of past manipulations [31]. Overall, several craquelures unfolded on the painting, furrowing both the ground and the painted layers, thus constituting an obvious and widespread phenomenon of degradation. This eventually led to the detachment of fragments in some cases, leaving the bare canvas visible.

Therefore, special care must be taken when handling this artwork so as not to exponentially increase the number of lacunae.

In addition to cracks from local impacts, evidence of careless handling of the painting is provided by the presence of two small holes on the left side of the artwork that perforate both the painted and ground layers (Figure 4a,b).

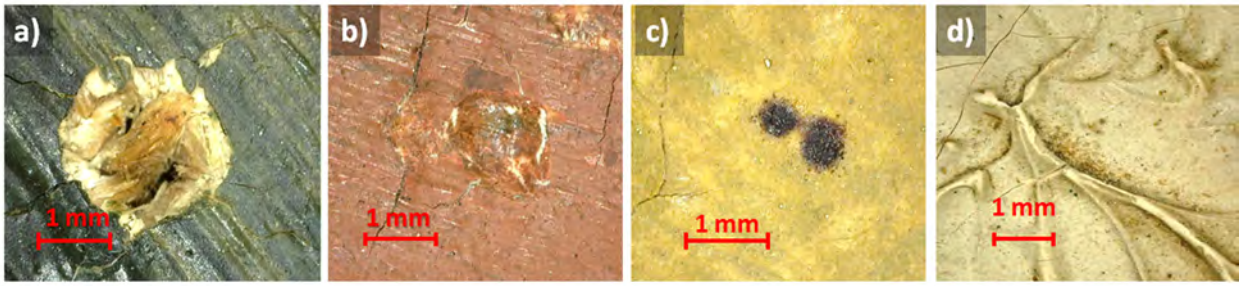

Figure 4. Microscopy photographs taken with Dino-lite instrumentation on (**a**) a small hole, (**b**) concavity, (**c**) stains from biological degradation, and (**d**) dust deposited on the folds of a thick brushstroke detected on the artwork.

The artwork is probably affected by a biological form of degradation, as small brown stains widely distributed over the painted surface were detected (Figure 4c). Dust and dirt naturally settled on the surface, particularly at the folds of the thick brushstrokes (Figure 4d). As with most twentieth-century paintings [37], it must be remembered that the painting was intentionally unvarnished, thus more prone to environmental depositions.

3.2. Painting Technique

Looking at the paint strokes, it can be seen that Andreina Rosa had probably laid down the paint using different brushes and amounts of color. Raking light observations helped accentuate the contrast between heavy and delicate brushstrokes. While the former type gave rise to noticeable bumps that cast shadows on the surroundings, the latter could barely be distinguished from the background in terms of thickness (Figure 5). All of the brushstrokes appear to be quite firm, suggesting that confident, quick, and intuitive movements were used. IR reflectography images also highlight such an attitude: it was revealed that only a single mark was located beneath the visible painted surface (Figures 5c and 6b). This might be considered as a *pentimento*, but is more likely to be just an oversight as such detail is not crucial for the final representation. No underlying drawing could be detected by IR reflectography: the lack of a preparatory sketch would be in agreement with the present reasoning, however, the opposite cannot be ruled out, since Andreina Rosa might have used a drawing material that does not absorb in the IR range employed and is therefore invisible [38]. The UV-induced fluorescence image of the artwork (Figure 6c) can be helpful to better see how the color was spread on the surface and to notice similarities or differences between paints.

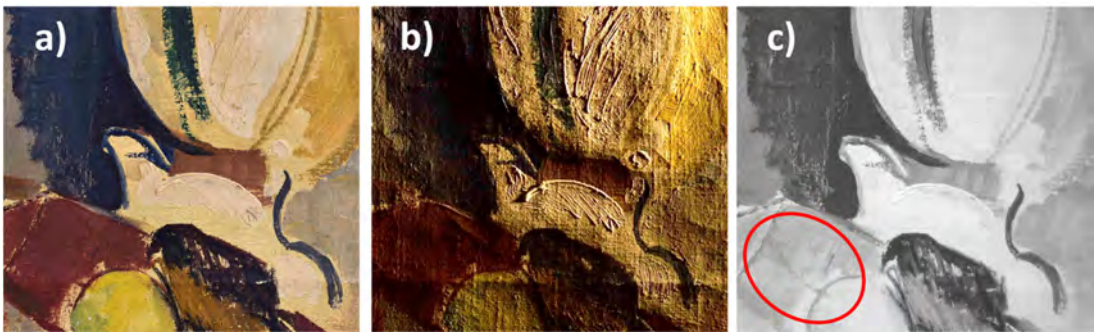

Figure 5. Detail of a central area of the painting where different kinds of brushstrokes can be observed. It is shown under conditions of (**a**) natural diffused light, (**b**) racking light, and (**c**) IR 950 filter. The last image reveals a pentimento, circled in red.

Figure 6. (**a**) Visible light, (**b**) IR reflectography (950 nm high-pass filter) with pentimento circled in red, and (**c**) UV-induced fluorescence images of the entire painting.

3.2.1. Preparation Layer

The preparation layer of the painting partially passed over the canvas, resulting in irregular and rather extensive white patches on the back. This suggests that the canvas was not commercially primed, but rather done by a craftsman or, more likely, by the artist herself. Under UV illumination, such areas presented a characteristic orange fluorescence (Figure 7); this could result from the presence of lithopone, which is reported in the literature as fluorescing yellow-orange [39,40]. However, the observed color could be the result of mixing different compounds together or be caused by other substances characterized by similar behavior under UV light.

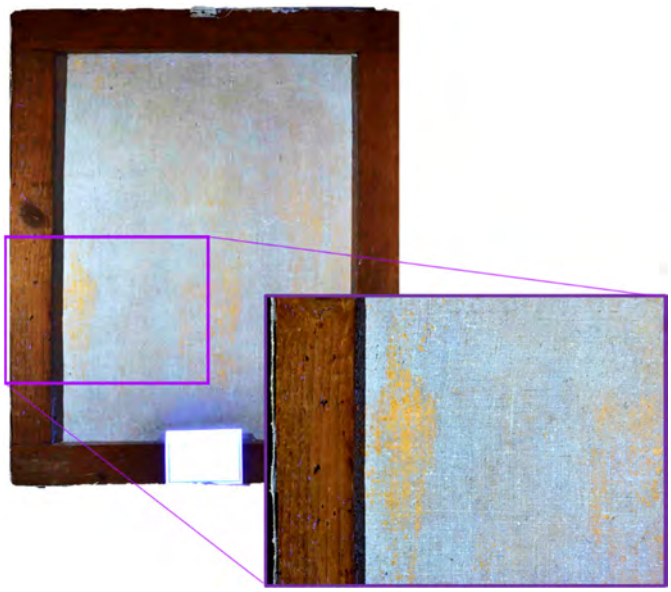

Figure 7. Photograph of the back of the painting taken under UV illumination. A detail of the area of interest is also shown.

Considering FORS spectra registered in different areas of the painting surface, it was possible to recognize the characteristic signals of gypsum and calcite, which are likely part of the ground layer but could be also present in the paint formulation as fillers (Figure 8).

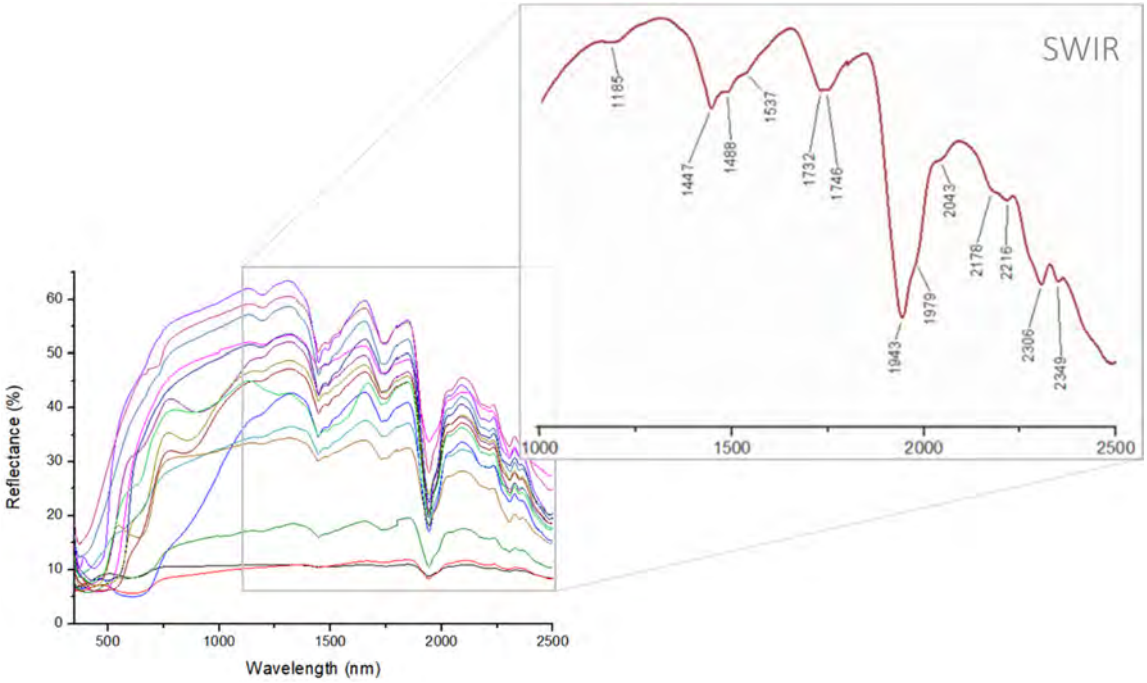

Figure 8. FORS spectra obtained for all the considered areas on the painting. On the right, a detail of the SWIR region, with spectral features common of all the acquisitions, clearly ascribable to gypsum.

The presence of gypsum, calcite, and animal glue in the grounding has been confirmed with Raman analyses. The response obtained for the preparation layer traversing the canvas (*Back*, Figure 9a) presented characteristic peaks for gypsum at 1008 cm^{-1} (SO_4 symm. str. [41]), calcite at 1090 cm^{-1} and lithopone at 986, 462 and 350 cm^{-1}. The possibility that zinc oxide is present in the preparation cannot be excluded, as a shoulder was detected at 436 cm^{-1} [4,42]. Nevertheless, since such signal was quite weak and could consist just of instrumental noise, the present observation was not considered as diagnostic but had to be supported by further evidence. The presence of an animal glue was attested by the typical features of this proteinaceous material (2980 ÷ 2880, 1446, 1378, 1332, 1598, 1248, 1122, 878 cm^{-1}) [43–45]. When the spectra obtained for the front of the artwork were considered, signals from the grounding could still be recognized, particularly where the painted layer was fairly thin (Figure 9b).

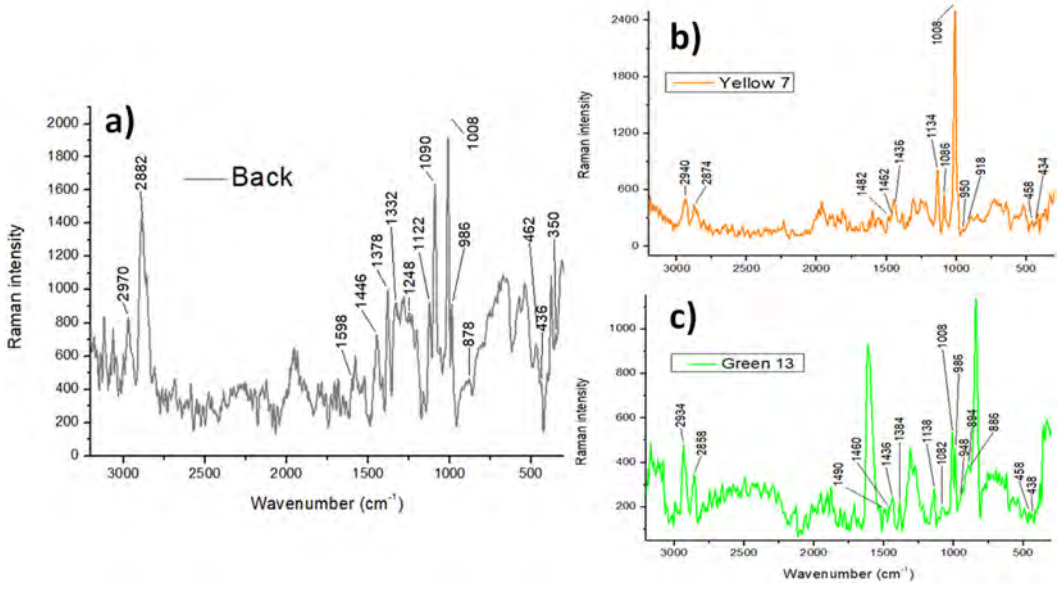

Figure 9. Raman spectra registered for (**a**) the preparation layer traversing the canvas (Back), (**b**) Yellow 7, and (**c**) Green 13.

Spectra obtained with ER-FTIR further confirmed the hypothesized composition of the grounding, as characteristic features for gypsum [41,46–50], calcite [46,51,52], lithopone [47,48,53,54], and for the proteinaceous glue [49,55–57] were registered (Figure 10b). Zinc oxide was also detected [53]. The components of the preparation layer also emerged on the IR spectra obtained for the painted surface (Figure 10c), as observed before for Raman analysis.

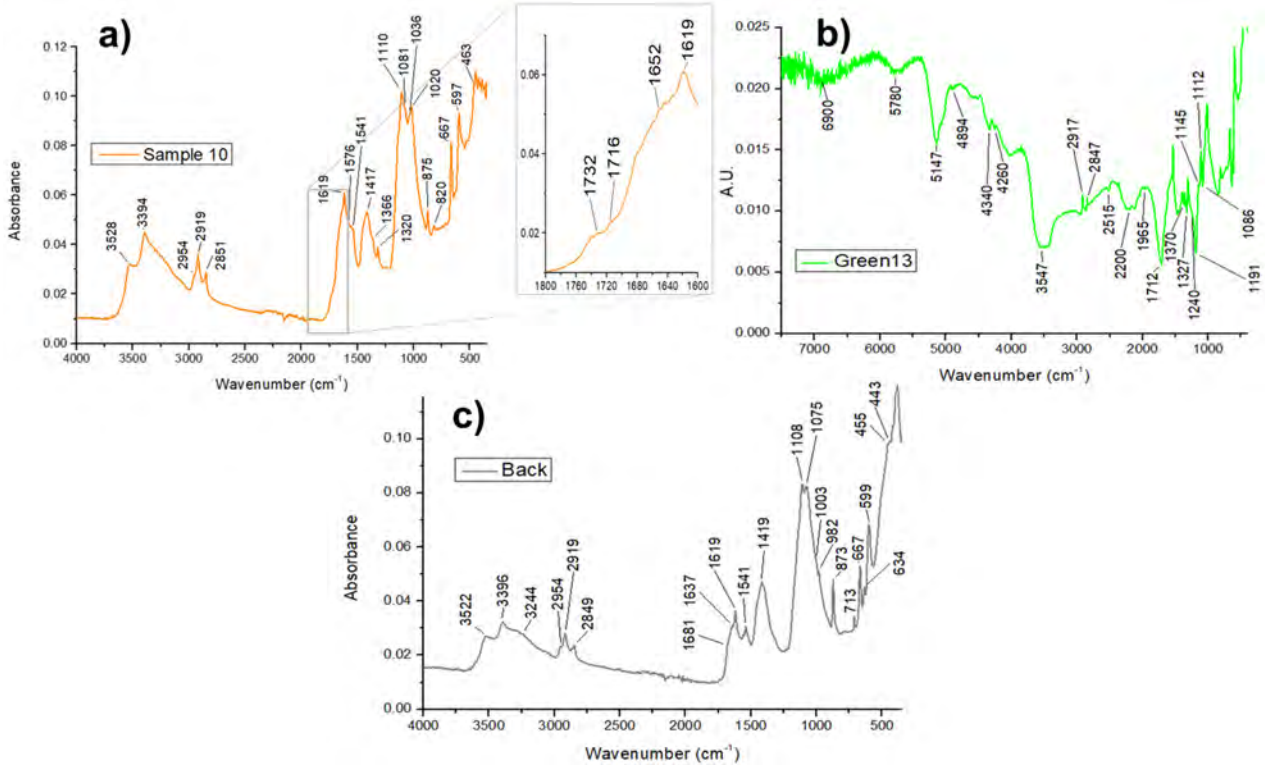

Figure 10. (**a**) ATR-FTIR spectrum registered for the yellow painted side of Sample 10 with detail of the signals in the region 1800–1600 cm^{-1}; (**b**) ER-FTIR spectrum obtained for Green 13; (**c**) ATR-FTIR spectrum of the back side of one of the samples (for all of them the signals registered coincided).

3.2.2. Paint Medium and Degradation Products

Based on the multi-analytical approach, the binder was found to be a dryingoil.

As for FORS results (Figure 8), the lipidic strongest absorption features in the 1200–2500 nm region were observed [58].

For all the analysed areas, Raman spectra presented a doublet in the region 2940 ÷ 2850 cm^{-1}; this was attributed to the C-H stretching modes of the organic binder [44].

ER-FTIR spectra of all the analyzed areas had characteristic features proper of lipidic binders too [49,50,59], as it can be seen in the spectrum for *Green 13* reported in Figure 10b. Furthermore, the lipidic binder is recognizable from the ATR spectra thanks to the characteristic triplet of signals at about 2954, 2920, and 2850 cm^{-1} given by the stretching of CH_2 and CH_3 groups [46,60,61]. The C=O stretching mode is associated with the shoulders at 1732 and 1716 cm^{-1} (shown in the detail of Figure 10a): the former is likely due to esters, whereas the latter to acids. Their trend can be explained according to what Mazzeo et al. observed on aged lipidic binders [60]: as the ageing proceeds, the ester band becomes broader due to the hydrolysis affecting triglycerides, while degradation products give rise to the second signal.

Raman and IR results allowed us to identify the presence of degradation products of linseed oil.

Mono- and di-hydrated forms of calcium oxalate, respectively named whewellite and weddellite, have been detected in Raman spectra (see Figure 9b,c). For the former,

diagnostic signals can be recognized at ca. 1490, 1460, 950 cm^{-1}, and in the range 886 ÷ 894 cm^{-1}, whereas the features at ca. 1440, 916, and 458 cm^{-1} are ascribable to the latter [62,63]. The calcium forming such salts likely derives from the calcite and the gypsum comprised in the grounding layer and/or present as fillers in paint formulations. Other metallic ions contained in the pigments have probably formed additional kinds of oxalates, which may be the reason for the several peaks and shoulders at wavenumbers similar to the ones described. Several studies underline the presence of these degradation products in other artworks, yet their formation mechanism is still not completely understood [63–66]. For the present painting by Andreina Rosa, both the biological degradation and the chemical alteration of oils through the formation of metal soaps, prior than oxalates, may have played a crucial role. The former phenomenon has probably affected the painting, giving rise to visible dark spots: the metabolism of microorganisms such as fungi, bacteria, and algae includes the secretion of oxalic acid [47,48]. Furthermore, the contribution of polluted urban air is not to be excluded from the possible factors that lead to the formation of oxalates, as the canvas has been stored in a private house, exposed to uncontrolled environmental conditions.

The presence of oxalates was confirmed by FTIR spectroscopy techniques, both in ER and ATR mode (Figure 10a,b). The C-O symmetric stretching of metal oxalates is probably the reason for the doublet at ca. 1370 and 1327 cm^{-1} detected in ER-FTIR spectra [67], and at ca. 1366 and 1320 cm^{-1} observed with ATR-FTIR [66,68]. In addition, weddellite and whewellite are likely contributing to the band observed in the range 1700 ÷ 1600 cm^{-1} registered through the latter spectroscopic technique, with features at ca. 1650 and 1620 cm^{-1} respectively [68].

ATR-FTIR measurements allowed also for the detection of metal soaps; these did not result in the characteristic aggregates and eruptions but are likely homogeneously distributed throughout the paint layers [69]. Carboxylic acids may have derived from oil ageing and have combined with alkaline earths or heavy metals present in the artwork, resulting in metal soaps [70–72]. On the other hand, metal soaps might have been part of the commercial paints formulations with the purpose of better dispersing the pigments in the medium or of lowering the price of the product [70,71]. Signals ascribable to the presence of calcium or zinc soaps (palmitates, stearates, or azelates) lie in the region between 1580 and 1576 cm^{-1} and around 1540 cm^{-1} and are associated with the asymmetric stretching of COO^{-} groups [69,71]. In addition, the sides of the band at 1417 cm^{-1} present some shoulders probably because of the underlying signals of CH_2 bending of metal soaps in the region 1464 ÷ 1434 cm^{-1} and the COO^{-} symmetric stretching at about 1396 cm^{-1} [73].

Further information about the organic components present in the painted layer was gained through GC/MS analyses, which were performed on a white-ochre, a light green, and a dark blue fragment, the former detached from the right side, and the others along the upper border of the canvas. The results showed the typical profile of (dried) drying oils: in the chromatograms it was possible to detect short and long-chain saturated monocarboxylic acids (such as nonanoic, lauric, myristic, palmitic, stearic, arachidic, and behenic acids); saturated dicarboxylic fatty acids (such as suberic, azelaic, and sebacic acids); minor amounts of unsaturated fatty acids (oleic acid); glycerol (see Figure 11 and Table 1). Besides dicarboxylic acids, other compounds indicate that an oxidation process had occurred and is still in progress: 3-oxo-1,8-octanedicarboxylic acid, cis-9,10-epoxy-octadecanoic, and 9,10-dihydroxy-octadecanoic acid.

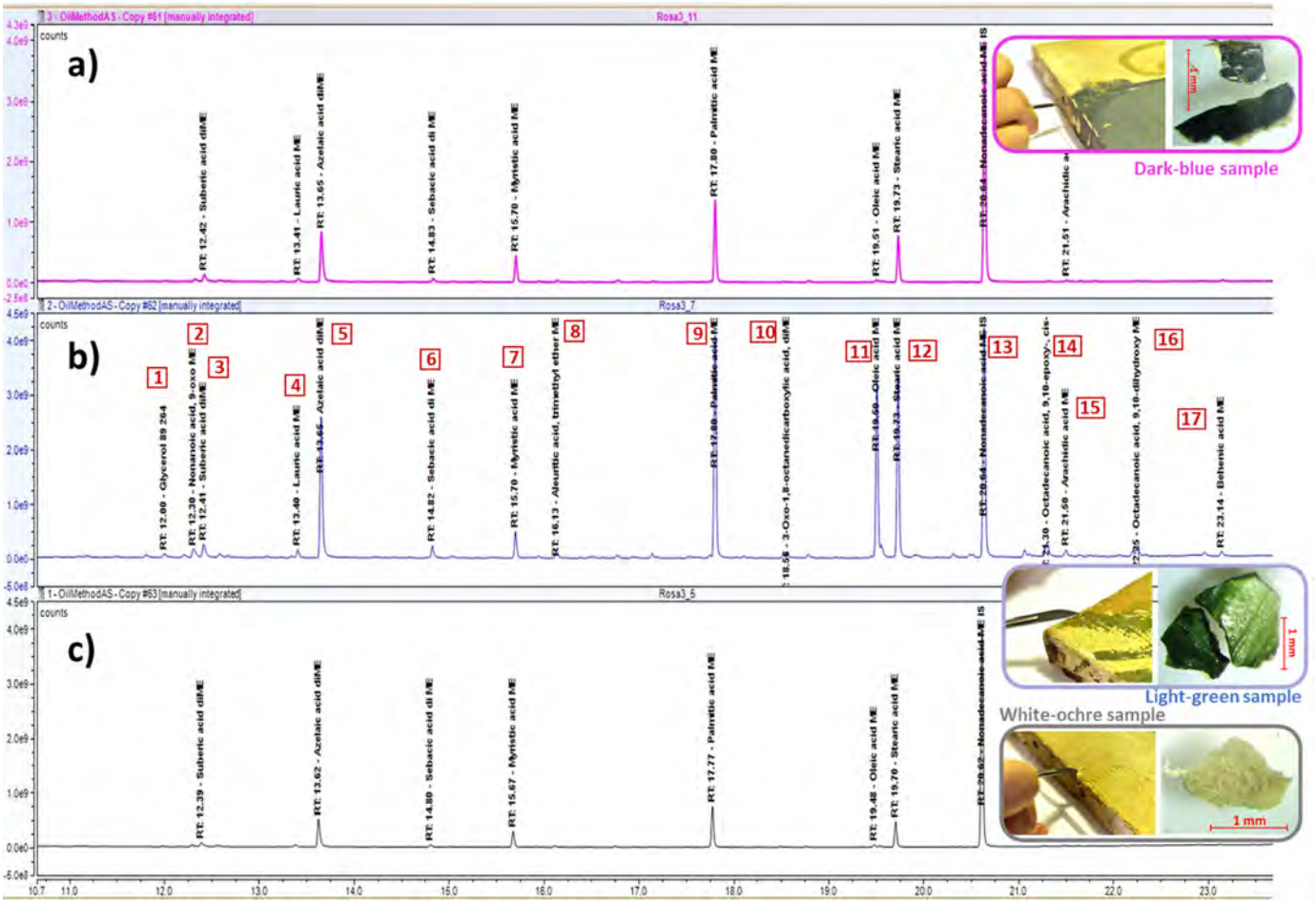

Figure 11. Total Ion Current (TIC) chromatograms after derivatization and analysis through GC-MS of (**a**) dark blue; (**b**) light green; and (**c**) white-ochre fragments. Ascending numbers are associated with the peaks in the chromatogram obtained for the green sample: the same ones are used in Table 1 to help data visualisation. Photographs of the sites of sampling and of the magnified fragments are shown too.

With curing and ageing, triglycerides present in fresh drying oils (rich in mono-, di-, and tri-unsaturated acids, respectively known as oleic, linoleic, and linolenic acid) undergo ruptures and fragmentations, giving rise to lower molecular weight-compounds such as hydroperoxides and peroxides. These are prone to form radicals and thus lead to the formation of aldehydes, ketones, and alcohols and eventually to dicarboxylic, dihydroxy, and hydroxylated monocarboxylic acids [10,24–26,70]. Since such oxidation products have been detected while linoleic or linolenic acids were not, it is possible to say the lipidic binders in the analyzed samples of the present painting underwent a substantial curing and ageing process. On the contrary, oleic acid is present in all the cases because its oxidation occurs more slowly compared to di- and tri- unsaturated fatty acids. Its content is quite low in the white-ochre and the dark blue fragments, so that the O/S ratio is 0.04 for the former and 0.02 for the latter, indicating a high level of maturity of the oil. In the green sample instead, the molar ratio between oleic and stearic acid is 0.94: this could be associated with the presence of zinc oxide, which was found to trap oleic acid in the painted layer by forming a packed structure [70,74]. The green color indeed probably contains ZnO, as suggested by spectroscopic analyses. Moreover, the thickness of the painted layer could have played a role in the curing and ageing of the green sample. Such a characteristic implies a slower ageing process since the oxygen availability is relatively lower.

Table 1. Retention times and attributions of the GC peaks registered for different samples.

Peak Number	Retention Time (min)	Attribution
1	11.998	Glycerol derivative
2	12.304	Nonanoic acid, 9-oxo methyl ester
3	12.413	Suberic acid dimethyl ester
4	13.403	Lauric acid methyl ester
5	13.651	Azelaic acid dimethyl ester
6	14.821	Sebacic acid dimethyl ester
7	15.698	Myristic acid methyl ester
8	16.130	Aleuritic acid, trimethyl ether methyl ester
9	17.804	Palmitic acid methyl ester
10	18.559	3-Oxo-1,8-octanedicarboxylic acid, dimethyl ester
11	19.552	Oleic acid methyl ester
12	19.729	Stearic acid methyl ester
13	20.637	Nonadecanoic acid methyl ester (Int.St.)
14	21.297	Octadecanoic acid, 9,10-epoxy-, cis-
15	21.501	Arachidic acid methyl ester
16	22.249	Octadecanoic acid, 9,10-dihydroxy methyl ester
17	23.137	Behenic acid methyl ester

With curing and ageing, triglycerides present in fresh drying oils (rich in mono-, di-, and tri-unsaturated acids, respectively known as oleic, linoleic, and linolenic acid) undergo ruptures and fragmentations, giving rise to lower molecular weight-compounds such as hydroperoxides and peroxides. These are prone to form radicals and thus lead to the formation of aldehydes, ketones, and alcohols and eventually to dicarboxylic, dihydroxy, and hydroxylated monocarboxylic acids [10,24–26,70]. Since such oxidation products have been detected while linoleic or linolenic acids were not, it is possible to say the lipidic binders in the analyzed samples of the present painting underwent a substantial curing and ageing process. On the contrary, oleic acid is present in all the cases because its oxidation occurs more slowly compared to di- and tri- unsaturated fatty acids. Its content is quite low in the white-ochre and the dark blue fragments, so that the O/S ratio is 0.04 for the former and 0.02 for the latter, indicating a high level of maturity of the oil. In the green sample instead, the molar ratio between oleic and stearic acid is 0.94: this could be associated with the presence of zinc oxide, which was found to trap oleic acid in the painted layer by forming a packed structure [70,74]. The green color indeed probably contains ZnO, as suggested by spectroscopic analyses. Moreover, the thickness of the painted layer could have played a role in the curing and ageing of the green sample. Such a characteristic implies a slower ageing process since the oxygen availability is relatively lower.

For all three samples, the molar ratios between azelaic and palmitic acids (A/P) resulted to be in the range 0.7–0.9, quite close to 1. These values support the hypothesis that a drying oil—and not egg—was used. Still, it is not possible to neglect the possibility that in other parts of the painting a different medium was employed since the samples considered are few and cannot be representative of the whole canvas. P/S ratios were calculated to be ca. 1.5, 1.3, and 1.7 for the white, green, and blue samples respectively, fairly similar to the one characteristic of linseed oil, 1.6 ± 0.3 [70].

3.2.3. The Color Palette

The similarity among many shades of colors present on the painting was questioned, aiming to better understand how the artist worked, whether she used mixtures of the same pigments, employed commercial paint tubes, or prepared her own recipes starting from raw materials. As a first approach, HIS was useful for assessing the resemblance of various hues. Figure 12 presents the color masks obtained for different endmembers where the pixels having a similar reflectance spectrum are evidenced with a false color. Additional information about the setting used can be found in Appendix C (Table 1).

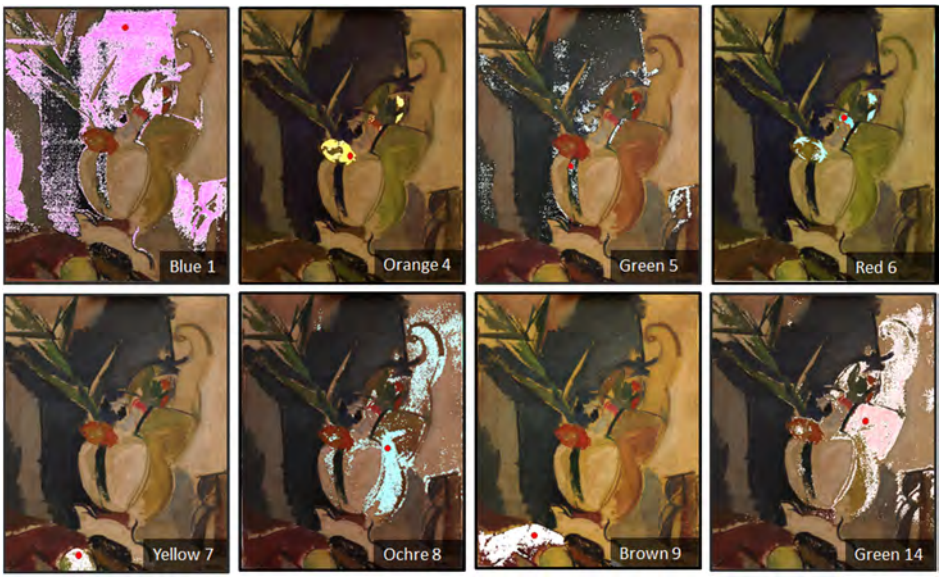

Figure 12. HIS masks obtained for chosen colour endmembers, selecting the points evidenced in red.

Blue shades could be grouped together and be related somehow to *Green 5*; similarities may be shared between *Orange 4* and *Red 6* and between *Ochre 8* with *Green 14;* whereas the two analyzed brown areas resulted very alike. *Yellow 7*, instead, could not be grouped with any other hue when considering HIS results. Other investigations demonstrated the pigments present in such a shade were actually widespread on many areas of the canvas.

The blue shades, together with the grey areas of the painting, are likely constituted by different mixtures of the same pigments: ultramarine blue, ivory black, and zinc white. With FORS, the characteristic reflection minimum of ultramarine blue in the region between 605 and 615 nm [16,75,76] has been detected (Figure 13). The low reflectance of the obtained spectra is due to the presence of a dark pigment, while the differences in relative intensity and position of the reflection minimum are ascribable to the variations in pigments proportions [76].

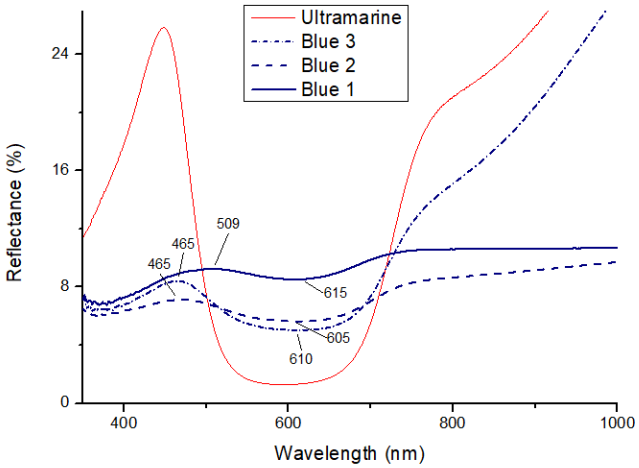

Figure 13. FORS spectra detail (350–1000 nm) registered for Blue 1, Blue 2, and Blue 3. The reference spectrum of synthetic ultramarine blue pigment is shown in red.

The presence of ultramarine blue pigment in Andreina Rosa's painting was confirmed also by Raman spectroscopy: the characteristic peak at ca. 546 cm^{-1} given by the symmetric stretching of S_3^- ions [53,75] was detected for all the analyzed blue areas. The two intense and broad peaks registered in the same spectra at 1604 and 1306 cm^{-1} are ascribable to the black pigment used in the mixture for obtaining the final dark greyish hue. This consists

probably of a carbon-based pigment, for which the former signal constitutes the so-called *G band*, and the latter the *D band* [77–83]. Moreover, a shoulder at ca. 962 cm^{-1} attributable to the phosphate (PO_4^{3-}) stretching suggests the black pigment could be ivory black [78,80]. *Blue 3* is considerably brighter than the other two and was probably mixed with a white pigment. This was possibly zinc white, whose characteristic signal at 434 cm^{-1} [4,42] was detected as a shoulder, next to the sharp peak at 414 cm^{-1} attributed to gypsum. *Blue 2* and *Blue 3* were also analyzed through ER-FTIR and the obtained spectra were characterized by strong *reststrahlen* peaks in the region between 1060 and 1020 cm^{-1}. These can be attributed to the Si, Al-O asymmetric stretching proper of ultramarine blue pigment [48]. The investigations carried out with ATR on a sample characterized by a blue shade similar to the one of *Blue 1*, resulted in a spectrum having characteristic peaks of both ultramarine blue and ivory black. The strong signals registered in the region 1063–1017 cm^{-1} are likely due to the Si-O stretching mode proper of the blue pigment [46,51,84], whereas the presence of ivory black was assessed thanks to the peaks given by the stretching modes of PO_4^{3-} at 879, 632, and 601 cm^{-1} [82]. Two further signs of evidence of the stretching of phosphate groups can be found in the shoulders at 562 and 470 cm^{-1}. Similar features were observed for a grey sample, as a confirmation of what was hypothesized based on HIS results. The presence of zinc white could be determined also for this color.

The FORS spectrum obtained for *Yellow 7* exhibited a good correspondence with a mixture of chrome yellow and zinc white in linseed oil (see Figure A3 in Appendix D). Such results were supported by Raman spectroscopy measurements as characteristic peaks of chrome yellow could be detected: the CrO_4^- stretching at 848 cm^{-1} and the Cr-O bending modes at 378, 358, 340, and 326 cm^{-1} [42,77,85]. The imperfect match in signal position and curve trend of the obtained spectrum with the ones reported in the literature may be ascribed to a slightly different crystal structure or formulation of the pigment [65] or the occurrence of some degradation phenomena involving the coloring agent based on the reduction of Cr^{VI} to Cr^{III} [66,85]. Such changes in the oxidation state of chrome have been observed to be possibly related to the formation of oxalates in a lipidic binder and likely cause a change of the color towards more greenish hues [66]. In the present painting, *Yellow 7* does appear to have a green shade and might thus be affected by the mentioned alteration phenomenon. Zinc white was detected by the Raman analysis since the characteristic peak at 434 cm^{-1} could be detected [4,42]. The ATR spectrum of a sample taken from the edge where the *Yellow 7* area was, had some correspondences with the reference spectra provided by the Institute of Chemistry University of Tartu (Estonia) [47] for chrome yellow, mainly in the signals at 1036, 597, and 463 cm^{-1}.

Raman analysis allowed us to detect chrome yellow and zinc white in *Ochre 8* and in the studied green shades. As the two pigments were always found together, they were likely part of the same commercial paint that the artist used for yellow hues. Goethite was probably included in *Ochre 8* as well, as suggested by the registered FORS spectrum. In the green colors, ultramarine blue and ivory black were detected too: these were probably mixed in different proportions to result in such distinct shades. Moreover, additional pigments might be present in the mixtures, as the registered instrumental responses were quite complex. For instance, the Raman spectrum of *Green 14* exhibited characteristic signals in the region 500–300 cm^{-1} that indicated the presence of some iron oxides or hydroxides of an earth pigment. FORS results suggested the presence of goethite in this color too.

Red 6 was hypothesized to be composed mainly of an iron-based pigment mixed with vermilion (see Figure A6).

Based on the FORS spectra registered for the red and orange colors, the similarity holding between them was assessed. For *Orange 4*, Raman spectroscopy revealed the presence of chrome yellow, while the signal registered at about 443 cm^{-1} with ER-FTIR analyses suggested hematite was present too [86]. Hence, the red color might be a commercial tube paint containing both vermilion and hematite.

Brown 9 and *10* have been found to be extremely similar. The presence of hematite in both was supported by the registered FORS spectra with characteristic s-shape and maxima at 620 and 750 nm and minimum at 880 nm, Raman signals at 415, 500, 615, 660, and 824 cm^{-1} [86] (see Figure A7) and ATR features at 470, 540, and 610 cm^{-1}.

Investigations on the whitish shades revealed that chrome yellow may also be present, as a maximum at 503 nm was registered in the derivative of the FORS spectra (see Figure A8): this was observed also in the analyzed yellow colors and was thus considered as a diagnostic feature. Weak signals related to such pigment were depicted also on the associated Raman spectra: the yellow component was probably included as a remnant of a previously used paint on the brush and was thus present in a low amount. Raman signals of lithopone were very strong instead, and were detected at 986, 646, 454, and 344 cm^{-1} (Figure 14) [53].

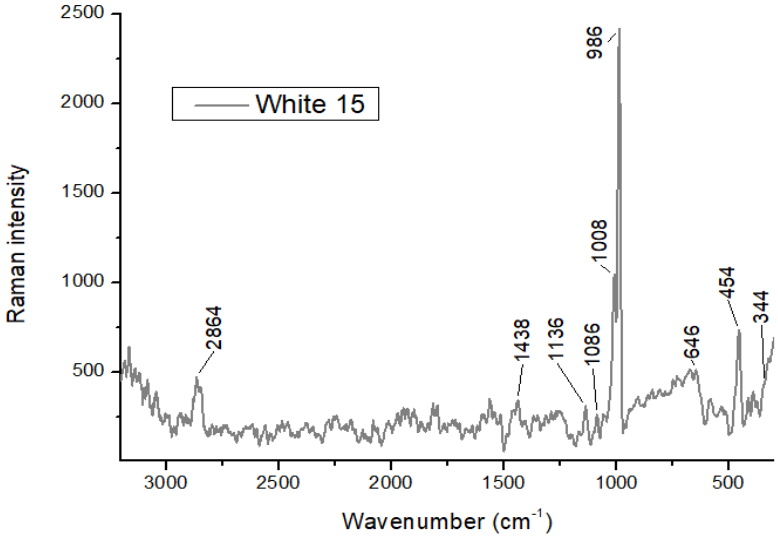

Figure 14. Raman spectrum registered for White 15.

This artwork visibly includes many different shades of color along the canvas: from the left side where there is a predominance of bluish and green tones, to the middle where intense reddish and ochre hues catch the eye, and to the right side with faded light-yellow tone, including the lower area colored mainly with browns.

In Table 2 the binding media, pigments, additives, and degradation products identified for the different analyzed areas are summarized. The reader shall be aware that the absence of certain compounds in some of the colors may not be due to an effective lack of such substances but related to the fact that not all the analytical techniques were performed for each considered area. Gypsum, calcium carbonate, and barium sulphate are reported as additives but may be actually part solely of the groundings, while metal soaps listed among the degradation products might also be additives of commercial paints.

Table 2. Binding media, pigments, additives, and degradation products identified through the multi-analytical study on the considered coloured areas of the artwork.

Area/Colour	Binding Media	Pigments	Inorganic Additives	Degradation Products	Comments
Grounding	Proteinaceous glue	-	Gypsum, chalk, lithopone, zinc oxide	-	Orange fluorescence under UV illumination

Table 2. *Cont.*

Area/Colour	Binding Media	Pigments	Inorganic Additives	Degradation Products	Comments
Blue 1	Lipidic material, more likely Linseed oil	Ultramarine blue, ivory black, zinc white	Gypsum, barium sulphate, calcite	Metal oxalates, weddelite, whewellite, metal soaps	
Blue 2				Metal oxalates	Hard to analyze with non-invasive technique due to its darkness
Blue 3				Metal oxalates, weddelite, whewellite	
Orange 4		Vermillion, hematite, chrome yellow		Metal oxalates	Low signals in Raman besides chrome yellow. In ER-FTIR derivative signals instead of peaks for metal oxalates
Green 5		Chrome yellow, ultramarine blue, zinc white, ivory black		Metal oxalates, whewellite, weddelite	
Red 6		hematite		Metal oxalates	Low signals in Raman besides chrome yellow. In ER-FTIR derivative signals instead of peaks for metal oxalates
Yellow 7		Chrome yellow, zinc white		Metal oxalates, whewellite, weddelite, metal soaps	
Ochre 8		Chrome yellow, zinc white, goethite			
Brown 9		Hematite			
Brown 10		Hematite, vermillion			
White 11		Lithopone, zinc white, chrome yellow		Metal oxalates, whewellite, weddelite, metal soaps.	
Grey 12		Ultramarine blue, ivory black, zinc white		Metal oxalates, whewellite, weddelite	
Green 13		Chrome yellow, ultramarine blue, zinc white, ivory black		Metal oxalates, whewellite, weddelite.	High variety and amount of oxidation products of the lipidic binder detected by GC-MS, probably slower ageing
Green 14				Metal oxalates, whewellite, weddelite	
White 15		Zinc white, chrome yellow		Metal oxalates	

4. Conclusions

By using a multi-analytical approach, the artistic materials and the painting technique used by Andreina Rosa for *Natura Morta* (1954–1955) and the painting state of conservation have been questioned. Based on the collected information, it was possible to infer the history of the painting: Andreina Rosa probably prepared the grounding herself and created her artwork on a bigger canvas compared to the actual size. Successively, the painting was re-dimensioned and transferred on new stretchers. The canvas was fixed to the wooden boards with nails and with the help of an adhesive; on the sides some paper was glued as a protection. The latter was then detached, causing extensive losses of paint.

The artwork was not in an optimal state of conservation, mainly ascribable to the transfer to the new wooden frame and to the uncontrolled environmental conditions during its storage. Evidences of this were the observed distortions, diffused cracking, and losses and a non-identified form of biological attack. Technical photography as well as microscopy observations helped in noticing and documenting such degradation phenomena with a completely non-invasive approach. The artwork has thus been assessed to be extremely fragile because of the widespread craquelures and the delicate balance that has established as a consequence of possible fluctuations in humidity levels. Hence, care must be taken in its handling and the environment of storage should be controlled (temperature and relative humidity oscillations). Furthermore, a mild consolidation treatment on the highly damaged sides could be helpful for the preservation of the painting integrity.

The crossing of information obtained both with macro- and microscopic observations and with different spectroscopic techniques allowed a compositional study of the preparation and painted layers. The former contain a very complex inorganic fraction, probably made of gypsum, lithopone, calcite, and zinc white, together with a proteinaceous glue. For the latter, Andreina Rosa has likely employed commercial oil-based paint tubes, containing mixtures of pigments as well as fillers and additives. Colouring agents such as ultramarine blue, chrome yellow, vermilion, and burnt sienna have been identified combining the information gained through complementary analytical tools like FORS, Raman, ER-FTIR, and ATR-FTIR spectroscopies. Such spectroscopic techniques also helped in the study of the organic fraction and GC-MS investigations corroborated the presence of a lipidic binder (most likely linseed oil). The quite advanced level of ageing of the binder was attested by the presence of a number of oxidation products, metal soaps, and oxalates. Nevertheless, the use of different binding media (such as egg yolk) could not be excluded with certainty: different formulations might have been employed throughout the canvas.

It is indeed widely affirmed that contemporary paintings are particularly complex to analyze as artists could, did, and still often do work with a multitude of possible materials, paint recipes, and techniques. Multi-analytical investigations constitute fundamental means of studying such complex mixtures, making it possible to provide more information about the artworks, their state of conservation, composition, and history. Since the studied painting constitutes a new acquisition for the International Gallery of Modern Art Ca' Pesaro, such knowledge points at the support for the outlining of adequate preservation policies as well as for the research on Andreina Rosa's artistic activity. Finally, given the lack of written records or interviews about her painting techniques, we hope to awaken curiosity about this Venetian artist and perhaps in the future we can count on testimonials from those who have worked with her/seen her in practice.

Author Contributions: Conceptualization, F.C.I. and E.B. (Elisabetta Barisoni); methodology, F.C.I., A.P., E.B. (Emanuele Bonato), L.F. and M.P.; investigation, F.C.I., A.P., E.B. (Emanuele Bonato), L.F. and P.L.-G.; data curation, F.C.I., A.P., E.B. (Emanuele Bonato), L.F. and P.L.-G.; writing—original draft preparation, F.C.I., A.P. and E.B. (Emanuele Bonato); writing—review and editing, F.C.I., A.P., E.B. (Emanuele Bonato), L.F., P.L.-G., E.B. (Eleonora Balliana) and D.C.; supervision, F.C.I.; project administration, F.C.I. and E.B. (Elisabetta Barisoni). All authors have read and agreed to the published version of the manuscript.

Funding: This research received no external funding.

Institutional Review Board Statement: Not applicable.

Informed Consent Statement: Not applicable.

Data Availability Statement: Not applicable.

Acknowledgments: This study was possible thanks to the research agreement between MUVE and the research group of "Heritage and Conservation Science" at the Ca' Foscari University. The authors want to thank G. Belli and P. Genovesi from MUVE for the fruitful collaboration. The authors would like to thank the Patto per lo Sviluppo della Città di Venezia (Comune di Venezia) for the support in the research.

Conflicts of Interest: The authors declare no conflict of interest.

Appendix A

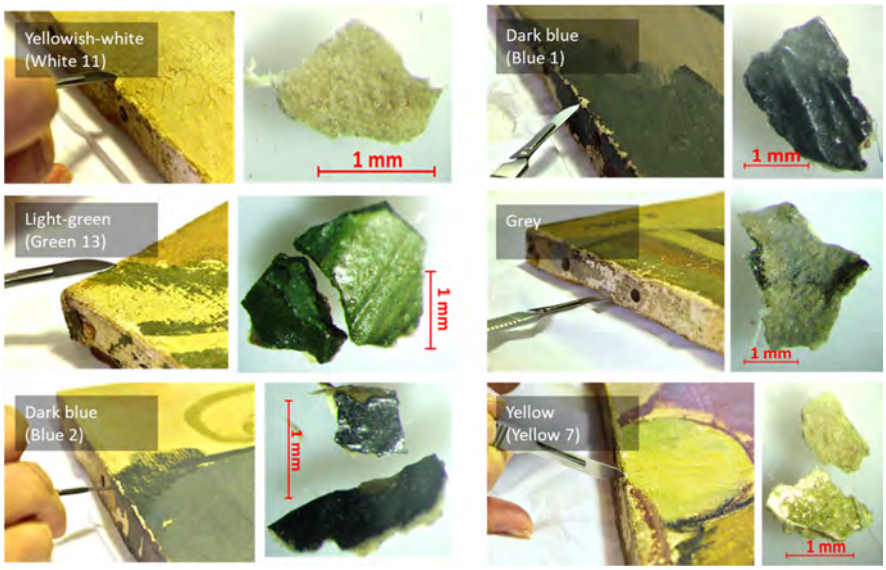

Figure A1. Detached areas and microscopical images of the fragments analyzed and cited in the text.

Appendix B

Figure A2. Areas analyzed with some spectroscopic techniques for the study of the glue present in different areas of the canvas and of the preparation layer. To each of them, a digital 55x magnification image is associated together with the assigned name.

Appendix C

Table 1. HIS masks reported in the paper, with the associated spectra and Pi.

Colour	Image	Spectrum
Blue 1	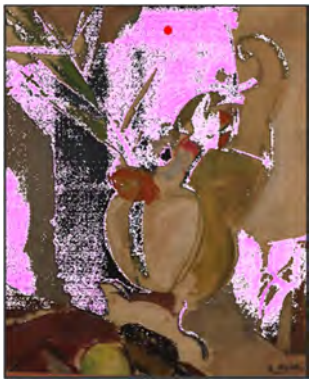	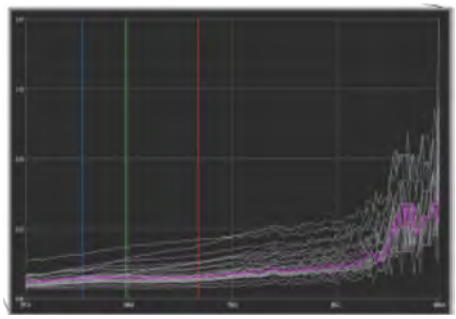 Pi = 0.09939
Yellow 7	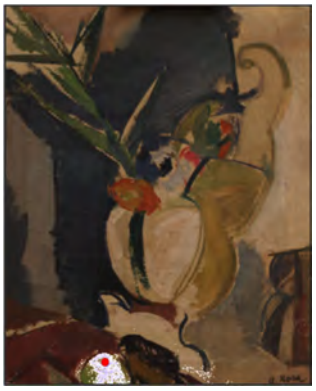	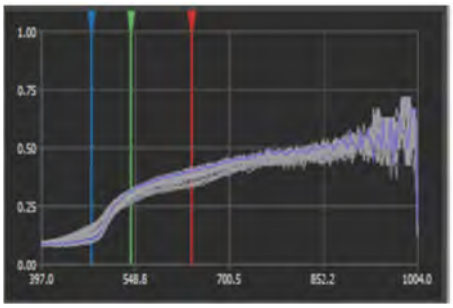 Pi = 0.9952
Ochre 8	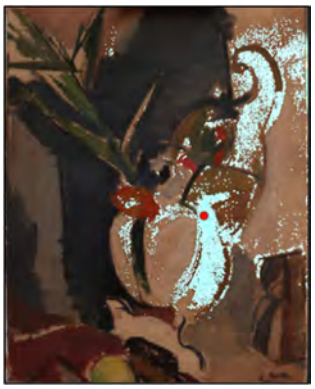	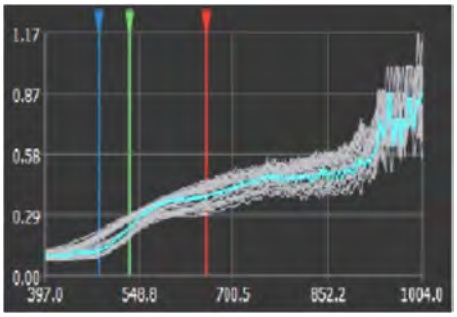 Pi = 0.9964
Green 5		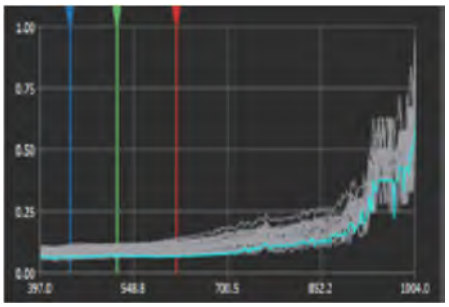 Pi= 0.9859

Table 1. *Cont.*

Colour	Image	Spectrum
Green 14	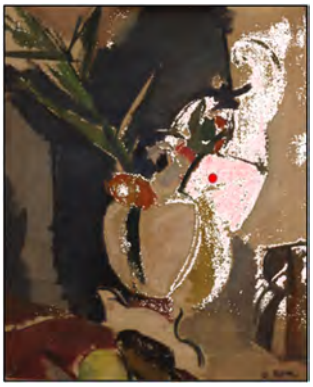	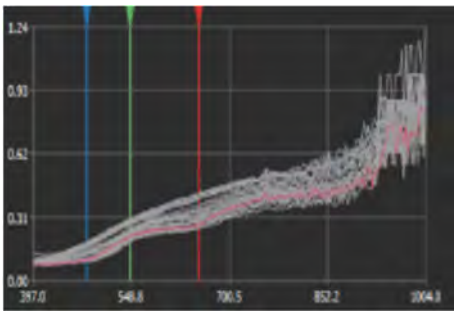 Pi = 0.9947
Red 6	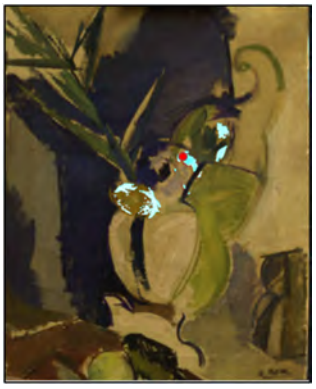	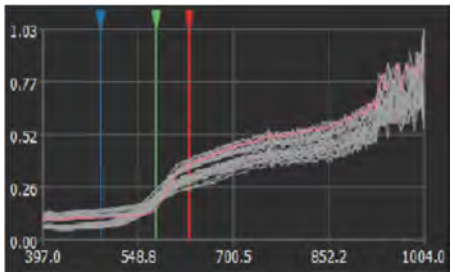 Pi = 0.9163
Orange 4	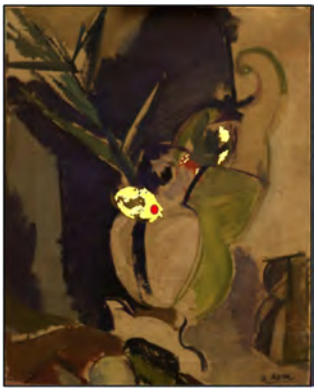	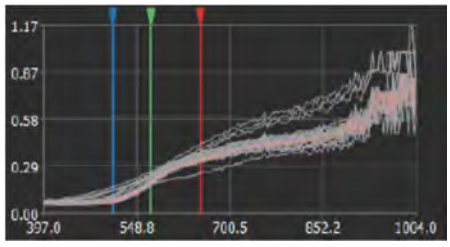 Pi = 0.9961
Brown 9		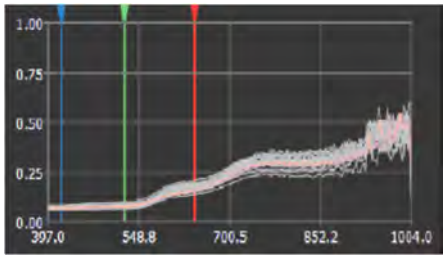 Pi = 0.9952

D.

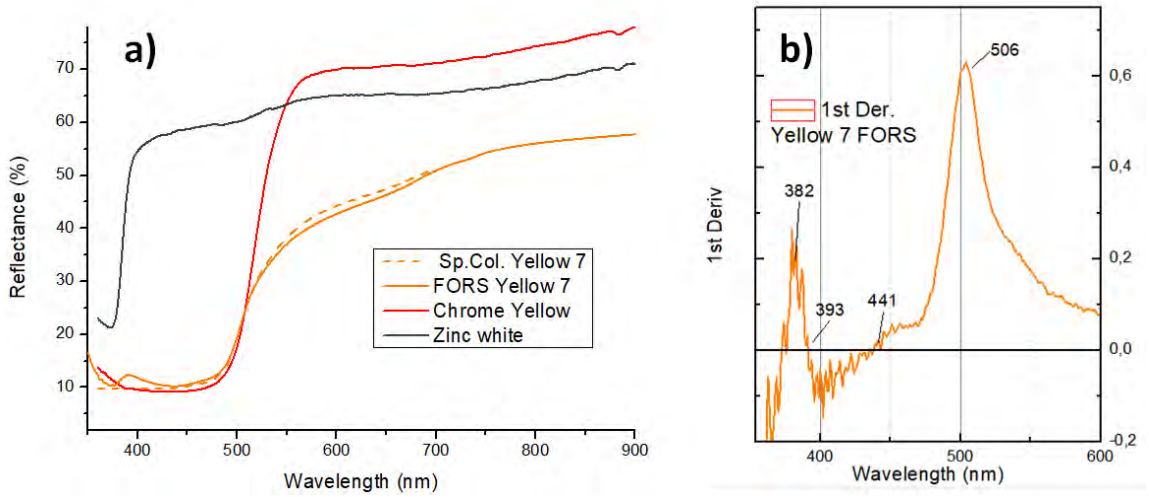

Figure A3. (**a**) Reflectance spectra obtained for Yellow 7 through FORS and using the Spectrocolorimeter (Sp.Col.). The reference FORS spectra of zinc white and Chrome Yellow are reported as well. (**b**) First derivative of the FORS spectrum for Yellow 7 in the region 354–600 nm, where characteristic features are labelled (maxima and null points of the derivative).

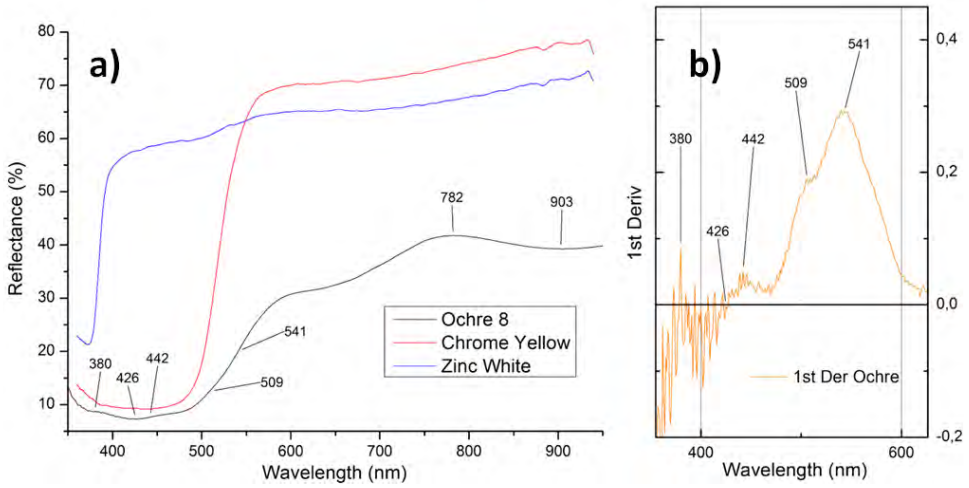

Figure A4. (**a**) Reflectance spectra obtained for Ochre 8 through FORS. The reference spectra of zinc white and Chrome Yellow are reported as well. (**b**) Detail of the first derivative of the FORS spectrum for Ochre 8, where characteristic features are labelled (maxima and null points of the derivative).

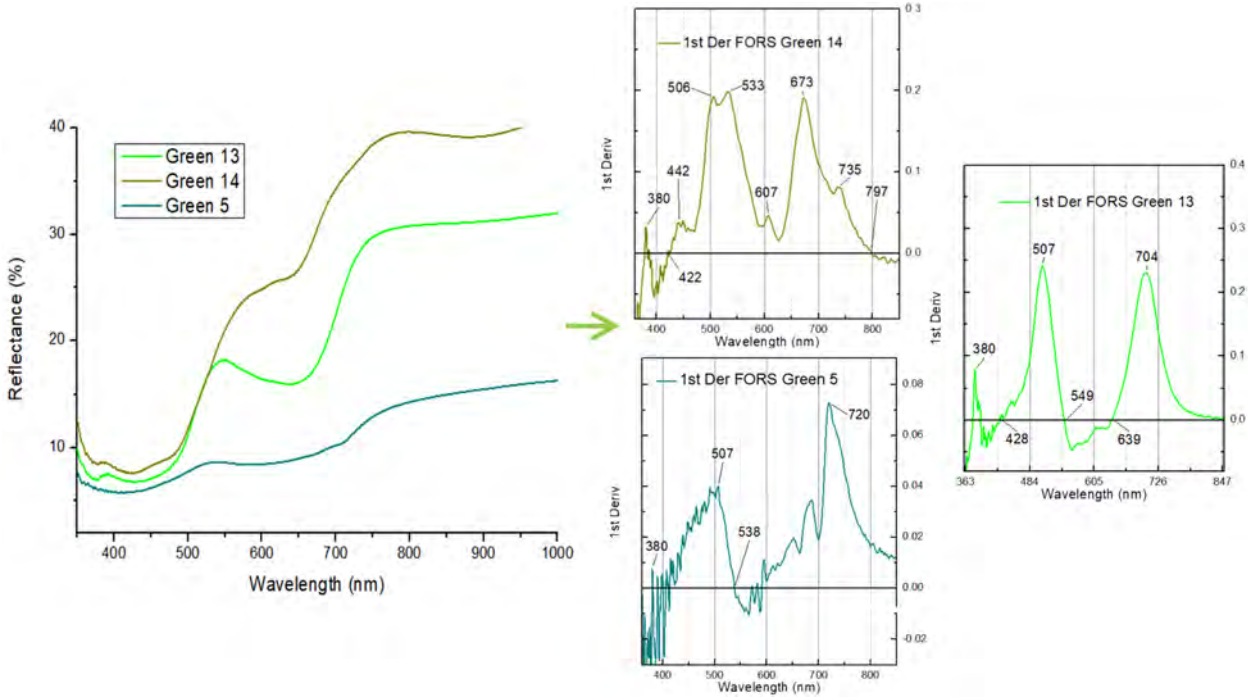

Figure A5. Reflectance spectra obtained through FORS for Green 5, Green 13, and Green 14 in the region 350–1000 nm. Details of the first derivative curves of the FORS spectra are also shown on the right side of the figure, where characteristic features are labelled (maxima and null points of the derivative).

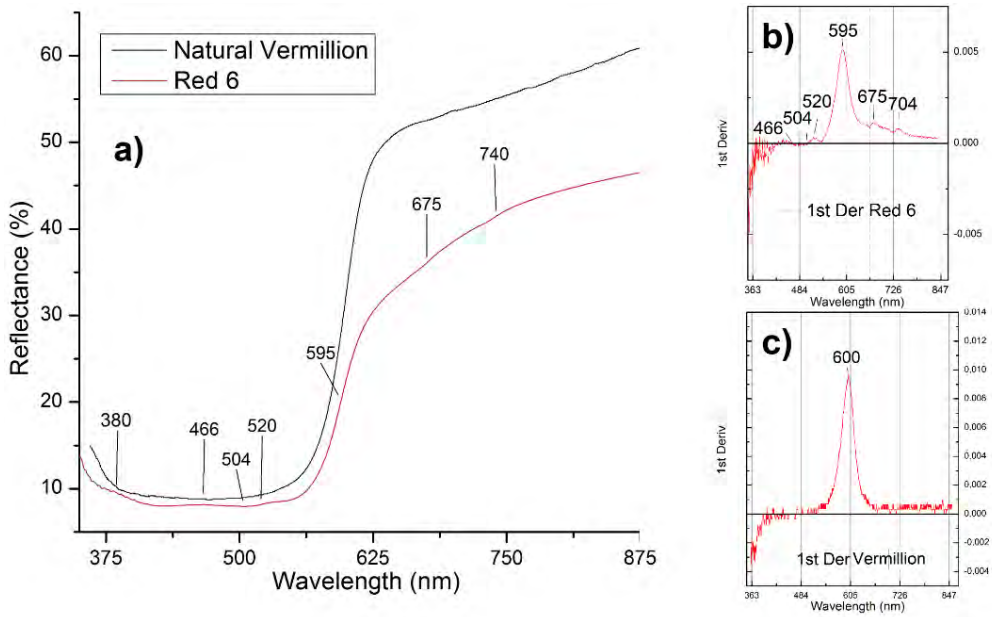

Figure A6. (**a**) Reflectance spectrum obtained through FORS for Red 6 in the region 350–900 nm in comparison with the one of natural vermilion. (**b**) Detail of the first derivative curve of the FORS spectrum of Red 6. (**c**) Detail of the first derivative curve of the FORS spectrum of natural vermilion, where characteristic features are labelled (maxima and null points of the derivative).

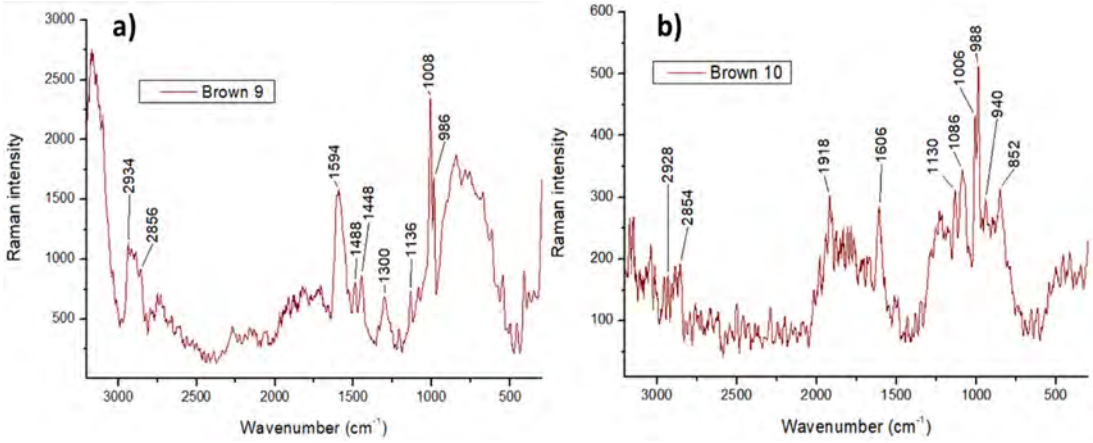

Figure A7. Raman spectra obtained for (**a**) Brown 9 and (**b**) Brown 10.

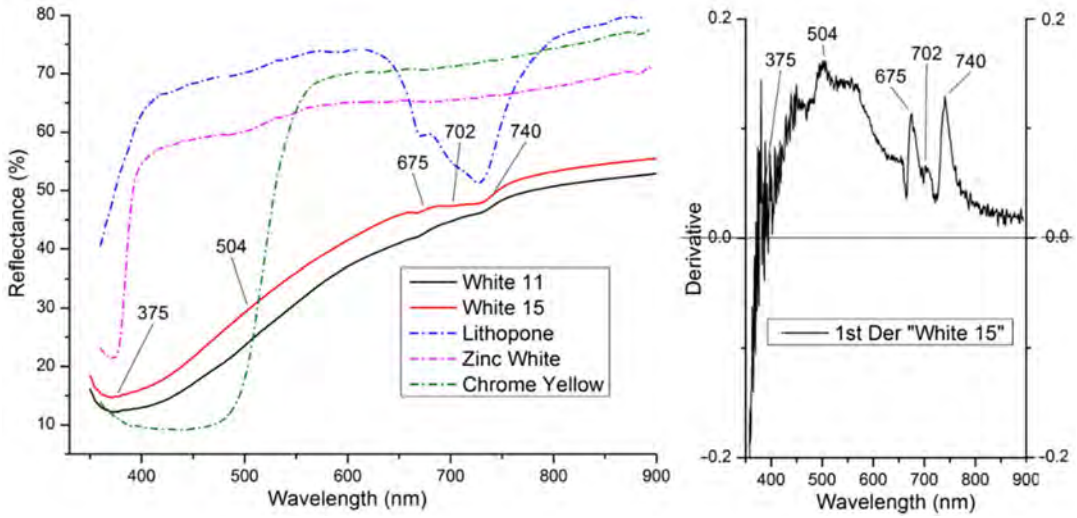

Figure A8. (**a**) FORS spectra of White 11 and 15 compared with zinc white, lithopone, and chrome yellow pigments; (**b**) first derivative of White 15 spectrum, where characteristic features are labelled (maxima and null points of the derivative).

References

1. Lutto nel Mondo Dell'arte Addio a Andreina Rosa. Available online: https://nuovavenezia.gelocal.it/venezia/cronaca/2019/07/09/news/lutto-nel-mondo-dell-arte-addio-a-andreina-rosa-1.36902949 (accessed on 6 March 2021).
2. Pavanello, G.; Stringa, N.; Baradel, V. (Eds.) *La Pittura Nel Veneto. Il Novecento*; Electa: Milano, Italy, 2006.
3. Izzo, F.C.; Ferriani, B.; den Berg, K.J.V.; Van Keulen, H.; Zendri, E. 20th Century Artists' Oil Paints: The Case of the Olii by Lucio Fontana. *J. Cult. Herit.* **2014**, *15*, 557–563. [CrossRef]
4. Giorgi, L.; Nevin, A.; Nodari, L.; Comelli, D.; Alberti, R.; Gironda, M.; Mosca, S.; Zendri, E.; Piccolo, M.; Izzo, F.C. In-Situ Technical Study of Modern Paintings Part 1: The Evolution of Artistic Materials and Painting Techniques in Ten Paintings from 1889 to 1940 by Alessandro Milesi (1856–1945). *Spectrochim. Acta Part A Mol. Biomol. Spectrosc.* **2019**, *219*, 530–538. [CrossRef]
5. Fuster-López, L.; Izzo, F.C.; Piovesan, M.; Yusá-Marco, D.J.; Sperni, L.; Zendri, E. Study of the Chemical Composition and the Mechanical Behaviour of 20th Century Commercial Artists' Oil Paints Containing Manganese-Based Pigments. *Microchem. J.* **2016**, *124*, 962–973. [CrossRef]
6. Carlesi, S.; Bartolozzi, G.; Cucci, C.; Marchiafava, V.; Picollo, M. The Artists' Materials of Fernando Melani: A Precursor of the Poor Art Artistic Movement in Italy. *Spectrochim. Acta Part A Mol. Biomol. Spectrosc.* **2013**, *104*, 527–537. [CrossRef] [PubMed]
7. Muir, K.; Gautier, G.; Casadio, F.; Vila, A. Interdisciplinary Investigation of Early House Paints: Picasso, Picabia and Their "Ripolin" Paintings. In *ICOM Committee for Conservation Preprints*; Bridgeland, J., Ed.; Critério-Artes Gráficas, Lda: Lisbon, Portugal, 2011; p. 23.
8. Muir, K.; Langley, A.; Bezur, A.; Casadio, F.; Delaney, J.; Gautier, G. Scientifically Investigating Picasso's Suspected Use of Ripolin House Paints in *Still Life*, 1922 and *The Red Armchair*, 1931. *J. Am. Inst. Conserv.* **2013**, *52*, 156–172. [CrossRef]
9. Izzo, F.C.; van den Berg, K.J.; van Keulen, H.; Ferriani, B.; Zendri, E. Modern Oil Paints—Formulations, Organic Additives and Degradation: Some Case Studies. In *Issues in Contemporary Oil Paint*; van den Berg, K.J., Burnstock, A., de Keijzer, M., Krueger, J., Learner, T., de Tagle, A., Heydenreich, G., Eds.; Springer International Publishing: Cham, Switzerland, 2014; pp. 75–104. [CrossRef]

10. Erhardt, D.; Tumosa, C.S.; Mecklenburg, M.F. Long-Term Chemical and Physical Processes in Oil Paint Films. *Stud. Conserv.* **2005**, *50*, 143–150. [CrossRef]
11. Bayliss, S.; van den Berg, K.J.; Burnstock, A.; de Groot, S.; van Keulen, H.; Sawicka, A. An Investigation into the Separation and Migration of Oil in Paintings by Erik Oldenhof. *Microchem. J.* **2016**, *124*, 974–982. [CrossRef]
12. Burnstock, A.; van den Berg, K.J.; de Groot, S.; Wijnberg, L. An Investigation of Water-Sensitive Oil Paints in 20th Century Paintings. In *Modern Paints Uncovered: Proceedings from the Modern Paints Uncovered Symposium, Getty Conservation Institute, London*; Learner, T., Smithen, J.W., Schilling, M.R., Eds.; Getty Conservation Institute: Los Angeles, CA, USA, 2006; pp. 177–188.
13. Cooper, A.; Burnstock, A.; van den Berg, K.J.; Ormsby, B. Water Sensitive Oil Paints in the Twentieth Century: A Study of the Distribution of Water-Soluble Degradation Products in Modern Oil Paint Films. In *Issues in Contemporary Oil Paint*; van den Berg, K.J., Burnstock, A., de Keijzer, M., Krueger, J., Learner, T., de Tagle, A., Heydenreich, G., Eds.; Springer International Publishing: Cham, Switzerland, 2014; pp. 295–310. [CrossRef]
14. Silvester, G.; Burnstock, A.; Megens, L.; Learner, T.; Chiari, G.; van den Berg, K.J. A Cause of Water-Sensitivity in Modern Oil Paint Films: The Formation of Magnesium Sulphate. *Stud. Conserv.* **2014**, *59*, 38–51. [CrossRef]
15. IFAC. Fiber Optics Reflectance Spectra (FORS) of Pictorial Materials in the 270–1700 nm Range. Available online: https://spectradb.ifac.cnr.it/fors/ (accessed on 20 April 2021).
16. U.S. Geological Survey. USGS Science for a Changing World. Available online: https://www.usgs.gov/labs/spec-lab (accessed on 21 April 2021).
17. Bacci, M.; Baronti, S.; Casini, A.; Lotti, F.; Picollo, M.; Casazza, O. Non-Destructive Spectroscopic Investigations on Paintings Using Optical Fibers. *MRS Proc.* **1992**, *267*, 265. [CrossRef]
18. Bacci, M.; Bellucci, R.; Cucci, C.; Frosinini, C.; Picollo, M.; Porcinai, S.; Radicati, B. Fiber Optics Reflectance Spectroscopy in the Entire VIS-IR Range: A Powerful Tool for the Non-Invasive Characterization of Paintings. *MRS Proc.* **2004**, *852*, OO2.4. [CrossRef]
19. Bacci, M.; Picollo, M.; Trumpy, G.; Tsukada, M.; Kunzelman, D. Non-Invasive Identification of White Pigments on 20Th-Century Oil Paintings by Using Fiber Optic Reflectance Spectroscopy. *J. Am. Inst. Conserv.* **2007**, *46*, 27–37. [CrossRef]
20. Fuster-López, L.; Izzo, F.C.; Damato, V.; Yusà-Marco, D.J.; Zendri, E. An Insight into the Mechanical Properties of Selected Commercial Oil and Alkyd Paint Films Containing Cobalt Blue. *J. Cult. Herit.* **2019**, *35*, 225–234. [CrossRef]
21. Caravá, S.; Roldán García, C.; Vázquez de Agredos-Pascual, M.L.; Murcia Mascarós, S.; Izzo, F.C. Investigation of Modern Oil Paints through a Physico-Chemical Integrated Approach. Emblematic Cases from Valencia, Spain. *Spectrochim. Acta Part A Mol. Biomol. Spectrosc.* **2020**, *240*, 118633. [CrossRef] [PubMed]
22. Källbom, A.; Nevin, A.; Izzo, F.C. Multianalytical Assessment of Armour Paints—The Ageing Characteristics of Historic Drying Oil Varnish Paints for Protection of Steel and Iron Surfaces in Sweden. *Heritage* **2021**, *4*, 1141–1164. [CrossRef]
23. Izzo, F.C.; Källbom, A.; Nevin, A. Multi-Analytical Assessment of Bodied Drying Oil Varnishes and Their Use as Binders in Armour Paints. *Heritage* **2021**, *4*, 3402–3420. [CrossRef]
24. Berg, J. *Analytical Chemical Studies on Traditional Linseed Oil Paints*; Molart Series; Netherlands Organization for Scientific Research: The Hague, The Netherlands, 2002.
25. Mills, J.S.; White, R. *The Organic Chemistry of Museum Objects*, 2nd ed.; First Issued in Hardback; Butterworth-Heinemann Series in Conservation and Museology; Routledge: London, UK; New York, NY, USA, 2015.
26. Colombini, M.P.; Modugno, F. (Eds.) *Organic Mass Spectrometry in Art and Archaeology*; Wiley: Chichester, UK, 2009.
27. Schilling, M.; Khanjian, H.; Carson, D.M. *Fatty Acid and Glycerol Content of Lipids*; Effects of Ageing and Solvent Extraction on the Composition of Oil Paints; Laboratoire de Recherche des Musées de France: Paris, France, 1997.
28. Asquier, M.; Colomban, P. Raman and Infrared Analysis of Glues Used for Pottery Conservation Treatments. *J. Raman Spectrosc.* **2009**, *40*, 1641–1644. [CrossRef]
29. Gorassini, A.; Adami, G.; Calvini, P.; Giacomello, A. ATR-FTIR Characterization of Old Pressure Sensitive Adhesive Tapes in Historic Papers. *J. Cult. Herit.* **2016**, *21*, 775–785. [CrossRef]
30. Vila, A.; Murray, A.; Andersen, C.K.; Izzo, F.C.; Fuster-López, L.; Aguado-Guardiola, E.; Jiménez-Garnica, R.; Scharff, A. Picasso 1917: An Insight into the Effects of Ground and Canvas in the Failure Mechanisms in Four Artworks. In *Conservation of Modern Oil Paintings*; van den Berg, K.J., Bonaduce, I., Burnstock, A., Ormsby, B., Scharff, M., Carlyle, L., Heydenreich, G., Keune, K., Eds.; Springer International Publishing: Cham, Switzerland, 2019; pp. 245–253. [CrossRef]
31. Fuster-López, L.; Izzo, F.C.; Andersen, C.K.; Murray, A.; Vila, A.; Picollo, M.; Stefani, L.; Jiménez, R.; Aguado-Guardiola, E. Picasso's 1917 Paint Materials and Their Influence on the Condition of Four Paintings. *SN Appl. Sci.* **2020**, *2*, 2159. [CrossRef]
32. Beninatto, R.; De Lucchi, O. *Chimica Organica per Artisti e Restauratori: Sostanze Naturali*; Createspace: Scotts Valley, CA, USA, 2016.
33. Dochia, M.; Sirghie, C.; Kozłowski, R.M.; Roskwitalski, Z. Cotton Fibres. In *Handbook of Natural Fibres*; Elsevier: Amsterdam, The Netherlands, 2012; pp. 11–23. [CrossRef]
34. Bratasz, Ł.; Vaziri Sereshk, M.R. Crack Saturation as a Mechanism of Acclimatization of Panel Paintings to Unstable Environments. *Stud. Conserv.* **2018**, *63*, 22–27. [CrossRef]
35. Giorgiutti-Dauphiné, F.; Pauchard, L. Painting Cracks: A Way to Investigate the Pictorial Matter. *J. Appl. Phys.* **2016**, *120*, 065107. [CrossRef]
36. Mathur, K.; Seyam, A.-F. Color and Weave Relationship in Woven Fabrics. In *Advances in Modern Woven Fabrics Technology*; Vassiliadis, S., Ed.; InTechOpen: London, UK, 2011. [CrossRef]

37. Burnstock, A.; van den Berg, K.J. Twentieth Century Oil Paint. The Interface between Science and Conservation and the Challenges for Modern Oil Paint Research. In *Issues in Contemporary Oil Paint*; van den Berg, K.J., Burnstock, A., de Keijzer, M., Krueger, J., Learner, T., de Tagle, A., Heydenreich, G., Eds.; Springer International Publishing: Cham, Switzerland, 2014; pp. 1–19. [CrossRef]
38. *Dalla Conservazione Alla Storia Dell'arte: Riflettografia e Analisi non Invasive per lo Studio Dei Dipinti*; Poldi, G.; Villa, G.C.F. (Eds.) Strumenti; Edizioni della Normale: Pisa, Italy, 2006.
39. Carden, M.L. Use of Ultraviolet Light as an Aid to Pigment Identification. *APT Bull.* **1991**, *23*, 26. [CrossRef]
40. Measday, D.; Victoria, M. A Summary of Ultra-Violet Fluorescent Materials Relevant to Conservation. Available online: https://aiccm.org.au/network-news/summary-ultra-violet-fluorescent-materials-relevant-conservation/ (accessed on 27 April 2021).
41. Knittle, E.; Phillips, W.; Williams, Q. An Infrared and Raman Spectroscopic Study of Gypsum at High Pressures. *Phys. Chem. Miner.* **2001**, *28*, 630–640. [CrossRef]
42. Bell, I.M.; Clark, R.J.H.; Gibbs, P.J. Raman Spectroscopic Library of Natural and Synthetic Pigments (Pre- ≈1850 AD). *Spectrochim. Acta Part A Mol. Biomol. Spectrosc.* **1997**, *53*, 2159–2179. [CrossRef]
43. Nevin, A.; Osticioli, I.; Anglos, D.; Burnstock, A.; Cather, S.; Castellucci, E. Raman Spectra of Proteinaceous Materials Used in Paintings: A Multivariate Analytical Approach for Classification and Identification. *Anal. Chem.* **2007**, *79*, 6143–6151. [CrossRef] [PubMed]
44. Nevin, A.; Osticioli, I.; Anglos, D.; Burnstock, A.; Cather, S.; Castellucci, E. The Analysis of Naturally and Artificially Aged Protein-Based Paint Media Using Raman Spectroscopy Combined with Principal Component Analysis. *J. Raman Spectrosc.* **2008**, *39*, 993–1000. [CrossRef]
45. Carlesi, S.; Becucci, M.; Ricci, M. Vibrational Spectroscopies and Chemometry for Nondestructive Identification and Differentiation of Painting Binders. *J. Chem.* **2017**, *2017*, 3475659. [CrossRef]
46. Stanzani, E.; Bersani, D.; Lottici, P.P.; Colomban, P. Analysis of Artist's Palette on a 16th Century Wood Panel Painting by Portable and Laboratory Raman Instruments. *Vib. Spectrosc.* **2016**, *85*, 62–70. [CrossRef]
47. Institute of Chemistry University of Tartu, Estonia. Database of ATR-FT-IR Spectra of Various Materials. Available online: https://spectra.chem.ut.ee/ (accessed on 13 April 2021).
48. Miliani, C.; Rosi, F.; Daveri, A.; Brunetti, B.G. Reflection Infrared Spectroscopy for the Non-Invasive in Situ Study of Artists' Pigments. *Appl. Phys. A* **2012**, *106*, 295–307. [CrossRef]
49. Rosi, F.; Daveri, A.; Moretti, P.; Brunetti, B.G.; Miliani, C. Interpretation of Mid and Near-Infrared Reflection Properties of Synthetic Polymer Paints for the Non-Invasive Assessment of Binding Media in Twentieth-Century Pictorial Artworks. *Microchem. J.* **2016**, *124*, 898–908. [CrossRef]
50. Rampazzi, L.; Brunello, V.; Corti, C.; Lissoni, E. Non-Invasive Techniques for Revealing the Palette of the Romantic Painter Francesco Hayez. *Spectrochim. Acta Part A Mol. Biomol. Spectrosc.* **2017**, *176*, 142–154. [CrossRef] [PubMed]
51. Bouchard, M.; Rivenc, R.; Menke, C.; Learner, T. Micro-FTIR and Micro-Raman Study of Paints Used by Sam Francis. *e-Preserv. Sci.* **2009**, *6*, 27–37.
52. Vahur, S.; Teearu, A.; Peets, P.; Joosu, L.; Leito, I. ATR-FT-IR Spectral Collection of Conservation Materials in the Extended Region of 4000-80 cm^{-1}. *Anal. Bioanal. Chem.* **2016**, *408*, 3373–3379. [CrossRef] [PubMed]
53. Burgio, L.; Clark, R.J.H. Library of FT-Raman Spectra of Pigments, Minerals, Pigment Media and Varnishes, and Supplement to Existing Library of Raman Spectra of Pigments with Visible Excitation. *Spectrochim. Acta Part A Mol. Biomol. Spectrosc.* **2001**, *57*, 1491–1521. [CrossRef]
54. Izzo, F.C.; Capogrosso, V.; Gironda, M.; Alberti, R.; Mazzei, C.; Nodari, L.; Gambirasi, A.; Zendri, E.; Nevin, A. Multi-Analytical Non-Invasive Study of Modern Yellow Paints from Postwar Italian Paintings from the International Gallery of Modern Art Cà Pesaro, Venice: Multi-Analytical Non-Invasive Study of Yellow Paints in Postwar Italian Paintings. *X-ray Spectrom.* **2015**, *44*, 296–304. [CrossRef]
55. Khatua, P.K.; Dubey, R.K.; Shahoo, S.C.; Kalawate, A. Environment Friendly, Exterior Grade Resin Adhesive from Phenol-Animal Glue Formaldehyde (PGF). *Int. J. Polym. Sci.* **2015**, *1*, 7.
56. Pellegrini, D.; Duce, C.; Bonaduce, I.; Biagi, S.; Ghezzi, L.; Colombini, M.P.; Tinè, M.R.; Bramanti, E. Fourier Transform Infrared Spectroscopic Study of Rabbit Glue/Inorganic Pigments Mixtures in Fresh and Aged Reference Paint Reconstructions. *Microchem. J.* **2016**, *124*, 31–35. [CrossRef]
57. Geweely, N.S.; Afifi, H.A.M.; Abdelrahim, S.A.; Alakilli, S.Y.M. Novel Comparative Efficiency of Ozone and Gamma Sterilization on Fungal Deterioration of Archeological Painted Coffin, Saqqara Excavation, Egypt. *Geomicrobiol. J.* **2014**, *31*, 529–539. [CrossRef]
58. Cloutis, E.; Norman, L.; Cuddy, M.; Mann, P. Spectral Reflectance (350–2500 Nm) Properties of Historic Artists' Pigments. II. Red–Orange–Yellow Chromates, Jarosites, Organics, Lead(–Tin) Oxides, Sulphides, Nitrites and Antimonates. *J. Near Infrared Spectrosc.* **2016**, *24*, 119–140. [CrossRef]
59. Invernizzi, C.; Rovetta, T.; Licchelli, M.; Malagodi, M. Mid and Near-Infrared Reflection Spectral Database of Natural Organic Materials in the Cultural Heritage Field. *Int. J. Anal. Chem.* **2018**, *2018*, 7823248. [CrossRef] [PubMed]
60. Mazzeo, R.; Prati, S.; Quaranta, M.; Joseph, E.; Kendix, E.; Galeotti, M. Attenuated Total Reflection Micro FTIR Characterisation of Pigment–Binder Interaction in Reconstructed Paint Films. *Anal. Bioanal. Chem.* **2008**, *392*, 65–76. [CrossRef] [PubMed]
61. van der Weerd, J.; van Loon, A.; Boon, J.J. FTIR Studies of the Effects of Pigments on the Aging of Oil. *Stud. Conserv.* **2005**, *50*, 3–22. [CrossRef]

62. Zoppi, A.; Lofrumento, C.; Mendes, N.F.C.; Castellucci, E.M. Metal Oxalates in Paints: A Raman Investigation on the Relative Reactivities of Different Pigments to Oxalic Acid Solutions. *Anal. Bioanal. Chem.* **2010**, *397*, 841–849. [CrossRef] [PubMed]
63. Rosado, T.; Gil, M.; Mirão, J.; Candeias, A.; Caldeira, A.T. Oxalate Biofilm Formation in Mural Paintings Due to Microorganisms—A Comprehensive Study. *Int. Biodeterior. Biodegrad.* **2013**, *85*, 1–7. [CrossRef]
64. Bordignon, F.; Postorino, P.; Dore, P.; Tabasso, M.L. The Formation of Metal Oxalates in the Painted Layers of a Medieval Polychrome on Stone, as Revealed by Micro-Raman Spectroscopy. *Stud. Conserv.* **2008**, *53*, 158–169. [CrossRef]
65. Otero, V.; Vilarigues, M.; Carlyle, L.; Cotte, M.; De Nolf, W.; Melo, M.J. A Little Key to Oxalate Formation in Oil Paints: Protective Patina or Chemical Reactor? *Photochem. Photobiol. Sci.* **2018**, *17*, 266–270. [CrossRef] [PubMed]
66. Simonsen, K.P.; Poulsen, J.N.; Vanmeert, F.; Ryhl-Svendsen, M.; Bendix, J.; Sanyova, J.; Janssens, K.; Mederos-Henry, F. Formation of Zinc Oxalate from Zinc White in Various Oil Binding Media: The Influence of Atmospheric Carbon Dioxide by Reaction with $13CO_2$. *Herit. Sci.* **2020**, *8*, 126. [CrossRef]
67. Monico, L.; Rosi, F.; Miliani, C.; Daveri, A.; Brunetti, B.G. Non-Invasive Identification of Metal-Oxalate Complexes on Polychrome Artwork Surfaces by Reflection Mid-Infrared Spectroscopy. *Spectrochim. Acta Part A Mol. Biomol. Spectrosc.* **2013**, *116*, 270–280. [CrossRef] [PubMed]
68. Cariati, F.; Rampazzi, L.; Toniolo, L. Calcium Oxalate Films on Stone Surfaces: Experimental Assessment of the Chemical Formation. *Stud. Conserv.* **2000**, *45*, 180–188.
69. Hermans, J.J.; Keune, K.; van Loon, A.; Iedema, P.D. An Infrared Spectroscopic Study of the Nature of Zinc Carboxylates in Oil Paintings. *J. Anal. At. Spectrom.* **2015**, *30*, 1600–1608. [CrossRef]
70. Izzo, F.C. 20th Century Artists' Oil Paints: A Chemical-Physical Survey. Ph.D. Thesis, Ca' Foscari University of Venice, Venezia, Italy, 2010.
71. Robinet, L.; Corbeil-a2, M.-C. The Characterization of Metal Soaps. *Stud. Conserv.* **2003**, *48*, 23–40. [CrossRef]
72. Izzo, F.C.; Kratter, M.; Nevin, A.; Zendri, E. A Critical Review on the Analysis of Metal Soaps in Oil Paintings. *ChemistryOpen* **2021**, *10*, 904–921. [CrossRef] [PubMed]
73. Otero, V.; Sanches, D.; Montagner, C.; Vilarigues, M.; Carlyle, L.; Lopes, J.A.; Melo, M.J. Characterisation of Metal Carboxylates by Raman and Infrared Spectroscopy in Works of Art: Characterisation of Metal Carboxylates by Raman and Infrared Spectroscopy in Works of Art. *J. Raman Spectrosc.* **2014**, *45*, 1197–1206. [CrossRef]
74. Osmond, G. Zinc White: A Review of Zinc Oxide Pigment Properties and Implications for Stability in Oil-Based Paintings. *AICCM Bull.* **2012**, *33*, 20–29. [CrossRef]
75. González-Cabrera, M.; Arjonilla, P.; Domínguez-Vidal, A.; Ayora-Cañada, M.J. Natural or Synthetic? Simultaneous Raman/Luminescence Hyperspectral Microimaging for the Fast Distinction of Ultramarine Pigments. *Dye. Pigment.* **2020**, *178*, 108349. [CrossRef]
76. Aceto, M.; Agostino, A.; Fenoglio, G.; Picollo, M. Non-Invasive Differentiation between Natural and Synthetic Ultramarine Blue Pigments by Means of 250–900 Nm FORS Analysis. *Anal. Methods* **2013**, *5*, 4184. [CrossRef]
77. Brooke, C.; Edwards, H.; Vandenabeele, P.; Lycke, S.; Pepper, M. Raman Spectroscopic Analysis of an Early 20th Century English Painted Organ Case by Temple Moore. *Heritage* **2020**, *3*, 1148–1161. [CrossRef]
78. Tomasini, E.P.; Halac, E.B.; Reinoso, M.; Di Liscia, E.J.; Maier, M.S. Micro-Raman Spectroscopy of Carbon-based Black Pigments. *J. Raman Spectrosc.* **2012**, *43*, 1671–1675. [CrossRef]
79. Stuart, B.H. *Analytical Techniques in Materials Conservation*; John Wiley & Sons: Hoboken, NJ, USA, 2007.
80. Coccato, A.; Jehlicka, J.; Moens, L.; Vandenabeele, P. Raman Spectroscopy for the Investigation of Carbon-Based Black Pigments: Investigation of Carbon-Based Black Pigments. *J. Raman Spectrosc.* **2015**, *46*, 1003–1015. [CrossRef]
81. Conti, C.; Botteon, A.; Bertasa, M.; Colombo, C.; Realini, M.; Sali, D. Portable Sequentially Shifted Excitation Raman Spectroscopy as an Innovative Tool for in Situ Chemical Interrogation of Painted Surfaces. *Analyst* **2016**, *141*, 4599–4607. [CrossRef] [PubMed]
82. Daveri, A.; Malagodi, M.; Vagnini, M. The Bone Black Pigment Identification by Noninvasive, In Situ Infrared Reflection Spectroscopy. *J. Anal. Methods Chem.* **2018**, *2018*, 6595643. [CrossRef] [PubMed]
83. Castro, K.; Pérez-Alonso, M.; Rodríguez-Laso, M.D.; Fernández, L.A.; Madariaga, J.M. On-Line FT-Raman and Dispersive Raman Spectra Database of Artists' Materials (e-VISART Database). *Anal. Bioanal. Chem.* **2005**, *382*, 248–258. [CrossRef] [PubMed]
84. Learner, T. *Analysis of Modern Paints*; Research in Conservation; Getty Conservation Institute: Los Angeles, CA, USA, 2004.
85. Monico, L.; Janssens, K.; Hendriks, E.; Brunetti, B.G.; Miliani, C. Raman Study of Different Crystalline Forms of $PbCrO_4$ and $PbCr_{1-x}S_xO_4$ Solid Solutions for the Noninvasive Identification of Chrome Yellows in Paintings: A Focus on Works by Vincent van Gogh: Raman Study of Different Crystalline Forms of $PbCrO_4$ and $PbCr_{1-x}S_xO_4$ Solid Solutions. *J. Raman Spectrosc.* **2014**, *45*, 1034–1045. [CrossRef]
86. Bikiaris, D.; Daniilia, S.; Sotiropoulou, S.; Katsimbiri, O.; Pavlidou, E.; Moutsatsou, A.P.; Chryssoulakis, Y. Ochre-Differentiation through Micro-Raman and Micro-FTIR Spectroscopies: Application on Wall Paintings at Meteora and Mount Athos, Greece. *Spectrochim. Acta Part A Mol. Biomol. Spectrosc.* **2000**, *56*, 3–18. [CrossRef]